A STUDY OF FIBER ORIENTATION IN PARTICLE-LOADED SUSPENSIONS USING A DIRECT SIMULATION METHOD WITH COLLISION STRATEGY

by

Xiaoqing Li

A thesis submitted to the Faculty of the University of Delaware in partial fulfillment of the requirements for the degree of Master of Science in Mechanical Engineering

Spring 2016

A STUDY OF FIBER ORIENTATION IN PARTICLE-LOADED SUSPENSIONS USING A DIRECT SIMULATION METHOD WITH COLLISION STRATEGY

by

Xiaoqing Li

Approved: ______________________________
Suresh G. Advani, Ph.D.
Professor in charge of thesis on behalf of the Advisory Committee

Approved: ______________________________
Suresh G. Advani, Ph.D.
Chair of the Department of Mechanical Engineering

Approved: ______________________________
Babatunde A. Ogunnaike, Ph.D.
Dean of the College of Engineering

Approved: ______________________________
Ann L. Ardis, Ph.D.
Senior Vice Provost for Graduate and Professional Education

ACKNOWLEDGMENTS

I would like to express my sincere gratitude to my most respected advisor, Dr. Suresh Advani. I'm greatly honored and fortunate to be one of your students. Thank you for all the help and encouragement along the way. I'm forever in debt to your priceless advice and guidance.

My deepest thanks go to Dr. Wook Ryol Hwang. He generously provided academic materials and numerical programs which made this work possible.

I would love to dedicate this work to my beloved family and friends, especially Xingchen Liu. You've all been nothing but supportive during my most difficult times. I think about every one of you all the time, even when we are oceans apart.

A heart-felt "thank you" to all the people who ever generously lent me a hand during the writing of this thesis.

TABLE OF CONTENTS

Appendix

LIST OF TABLES

LIST OF FIGURES

ABSTRACT

Short-fiber reinforced composite materials are widely in use in the manufacturing industries to bridge the property gap between continuous-fiber composites and unreinforced materials. Short-fiber composites can effectively strengthen the matrix materials along the fiber length direction, and can still be processed by highly-automated and economical methods such as injection or compression molding. It's essential to understand and predict the fiber orientation and its influence on the mechanical properties of the composite. However, the hydrodynamic interactions between the matrix and the fibers, and the inter-fiber interactions are not fully understood yet. Sometimes circular particles are added to the matrix for toughening and this may also influence the orientation of the short fibers during flow. In this thesis, we adopt a two-dimensional direct simulation method to investigate, for the first time, the effect of the presence of circular particles on the fiber orientation of short-fiber suspensions. To deal with the collision between fibers or fibers and particles, an ad-hoc method is proposed and developed. We predict the time-evolution of the elliptical fiber orientation as the volume fraction and aspect ratio increases, and compare it with that of the fiber-particle suspensions. The interaction coefficient C_I is calculated and compared with existing models. It is found that the presence of circular particles increases the rotary diffusion of a fiber suspension, and that, as the content of circular particles increases, the fiber alignment in the direction of shear is less pronounced.

Chapter 1

INTRODUCTION

1.1 Short-fiber Composite Materials

Short-fiber reinforced composite materials are widely in use in the manufacturing industries to bridge the property gap between continuous-fiber composites and unreinforced materials. Short-fiber composites can effectively strengthen the matrix materials along the fiber length direction, and can still be processed by highly-automated and economical methods such as injection or compression molding. It's essential to understand and predict the fiber orientation and its influence on the mechanical properties of the composite. However, the hydrodynamic interactions between the matrix and the fibers, and the inter-fiber interactions are not fully understood yet. Sometimes circular particles are added to the matrix for toughening and this may also influence the orientation of the short fibers during flow. In this thesis, we adopt a two-dimensional direct simulation method to investigate, for the first time, the effect of the presence of circular particles on the fiber orientation of short-fiber suspensions. To deal with the collision between fibers or fibers and particles, an ad-hoc method is proposed and developed. We predict the time-evolution of the elliptical fiber orientation as the volume fraction and aspect ratio increases, and compare it with that of the fiber-particle suspensions. The interaction coefficient C_I is calculated and compared with existing models. It is found that the presence of circular particles increases the rotary diffusion of a fiber suspension, and that, as the content of circular particles increases, the fiber alignment in the direction of shear is less pronounced.

Previous researchers have used phenomenological steady state shear flow experimental results to characterize a steady state value of C_I, but in this work, we will evaluate a time-dependent value of C_I which depends on the orientation state of the fibers. This work will focus on suspensions with both fibers and particles, and treat them discretely unlike other researchers who treat the matrix with the particles as a homogeneous suspension with an effective viscosity, to address the dynamics of fibers in the suspension. This assumption is reasonable when the particle diameter are much smaller than the fiber diameter.

Glass Fiber Reinforced Polymers (GFRPs) were introduced to improve the strength of the composites as the fibers shoulder much of the stress transferred from the polymer, and also slow down and even stop the propagation of the cracks in the matrix, therefore "reinforce" the polymer material.

Over the past few decades, the composite materials have played a significant role in applications ranging from defense to automotive to infrastructure to consumer products (Figure 1.1). The engineered composite family can be generally classified into the following categories: (a) composite building materials, (b) reinforced plastics, (c) metal composites, and (d) ceramic composites.

Reinforced plastics, generally referring to fiber-reinforced plastics, is a composite material made of a polymer matrix reinforced with fibers. Depending on the length of the fibers, they are further categorized into continuous fiber reinforced plastics (a.k.a. advanced composites), long fiber reinforced plastics, and short fiber reinforced plastics.

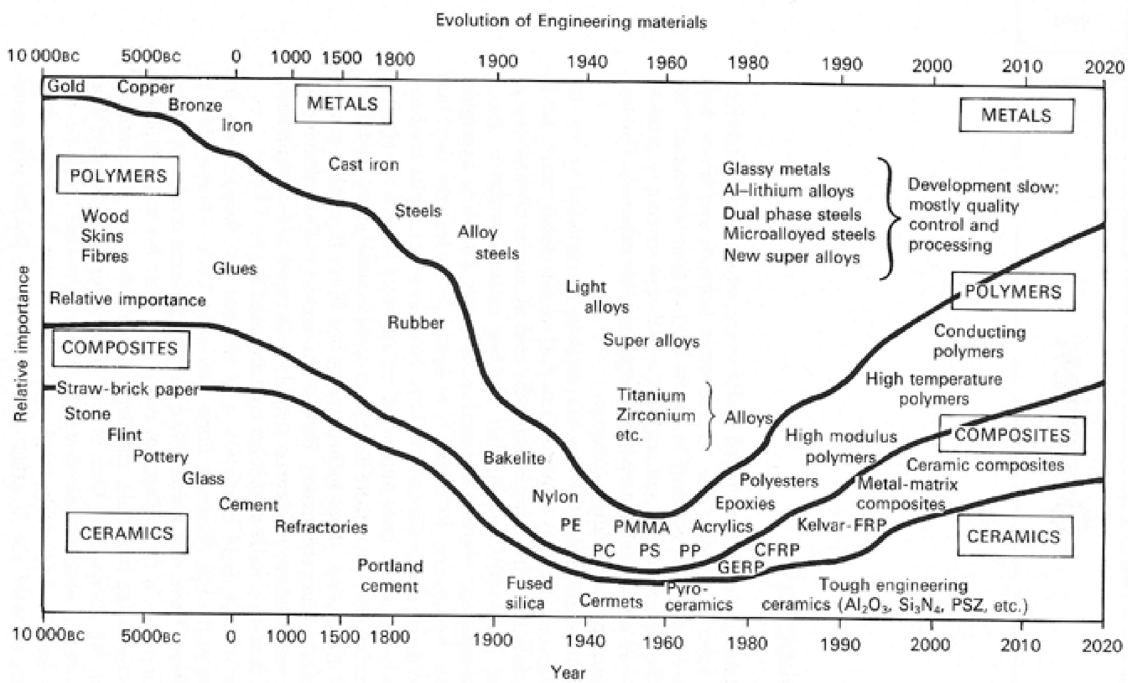

Figure 1.1: Schematic diagram showing the relative importance of the four classes of materials (ceramics, composites, polymers and metals). The time scale is nonlinear. (Reproduced with permission: Ashby, 1987. [1])

The three most common mass production processes for short fiber composites are injection molding, compression molding and extrusion. These processes were adopted from the polymer processing industry which had developed the equipment to produce parts in high volumes with polymers. Extrusion is a continuous process, injection molding is an automated process and compression molding is a semi-automated process but can manufacture large and complex parts which cannot be easily accomplished otherwise.

The fibers can be cut or chopped and compounded in an extruder with any polymer to form a pellet consisting of short fibers or could be pultruded consisting of aligned fibers. The pellets are usually a few centimeters in length and a few millimeters in diameter, as shown in Figure 1.2. Some typical short-fiber composite materials are listed in Table 1.1 [2].

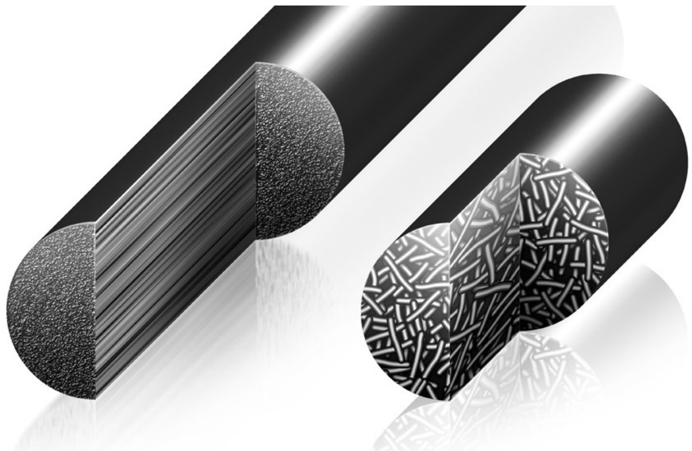

(a) Pultruded pellet with aligned fibers (*left*); Extruded pellet with short fibers (*right*).

(b) Continuous strands of fiber (*top*); Resulting long fiber reinforced thermoplastic pellets (*bottom*).

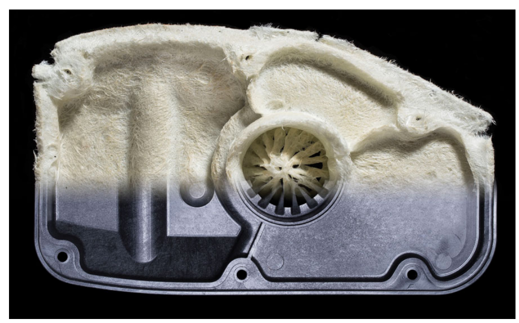

(c) Internal fiber skeleton of long-fiber reinforced composite part (*top-half*); Long-fiber reinforced composite part (*botttom-half*).

Figure 1.2: (a) A diagram of long- and short- fiber reinforced composite pellets; (b) An actual photo of fiber strands and resulting pellets; (c) An example of the injection-molded part compared with its fiber skeleton. (Reproduced with permission: PlastiComp, Inc. [3])

Table 1.1: A list of some typical polymer short-fiber materials. (Reproduced with permission: Tucker and Advani, 1994. [2])

Material	Processes	Matrix materials	Fiber materials	Fiber length (mm)	Fiber diameter (mm)	Fiber volume fraction	Concentration parameter cL/D
Short-fiber thermoplastics	injection molding, extrusion	Nylon, polycarbonate, many other thermoplastics	glass fiber, carbon fiber	0.2; wide distribution	0.013 (filaments)	0.05-0.20	0.7-3.0
Long-fiber thermoplastics	injection molding	Nylon, PEEK, LCP's, other thermoplastics	glass fiber, carbon fiber, aramid fiber	max. $\sim$1.3, some distribution	0.013 (filaments)	0.15-0.30	15-30
Sheet molding compound	compression molding	unsaturated polyesters	glass fiber, carbon fiber	25	$\sim$1 (bundles)	0.05-0.35	1.2-70
Bulk molding compound	injection molding	unsaturated polyesters	glass fiber	13	$\sim$1 (bundles)	0.05-0.25	0.6-3.2
Short-fiber glass mat thermoplastics (GMT)	compression molding	polypropylene, some other thermoplastics	Nylon, glass fiber mat	13	0.013 (filaments), some bundles	0.05-0.25	50-250
Long discontinuous fiber (LDF) prepregs	sheet forming	high-performance thermoplastics or thermosets	carbon fiber	150	$\sim$1 (tows or bundles)	0.40-0.60	60-90

The mechanical properties of a short-fiber composite are highly dependent on the fiber orientation, which evolves as the resin deforms in the manufacturing process and becomes part of the microstructure of the final part. Figure 1.3 shows the trends of the elasticity in three perpendicular directions as functions of the 1-direction orientation a_{11}, a measure of the level of fiber alignment to the 1-direction (see Eq. 2.14).

1.2 Hydrodynamics in Short-fiber Suspensions

In order to achieve the desired properties, the processing-induced fiber orientation must be properly predicted. However, this task is not easy, especially for more complex geometries.

There has been a considerable amount of research focusing on prediction of fiber orientation in flowing suspensions. Einstein [4] calculated the effective viscosity of a dilute suspension of spheres to be

$$\eta_r = 1 + 5\phi/2 + \Omega(\phi^2) \tag{1.1}$$

where $\eta_r = \eta/\eta_s$. Jeffery calculated the instantaneous angular velocity of a neutrally buoyant ellipsoid immersed in an infinite Newtonian medium undergoing Stokes flow [5]. An equivalent ellipsoid in simple shear flow was proved to be possible for nearly any body of revolution by Bretherton [6], and was determined for cylindrical fibers by Cox [7] and Harris and Pittman [8].

Batchelor [9] proposed a generalized stress system considering the hydrodynamics in a suspension, which was extended by Hinch and Leal [10]. Dinh and Armstrong [11] furthered the work and developed a constitutive equation to describe the rheological behavior of semiconcentrated suspensions, a correction term for its discrepancy from

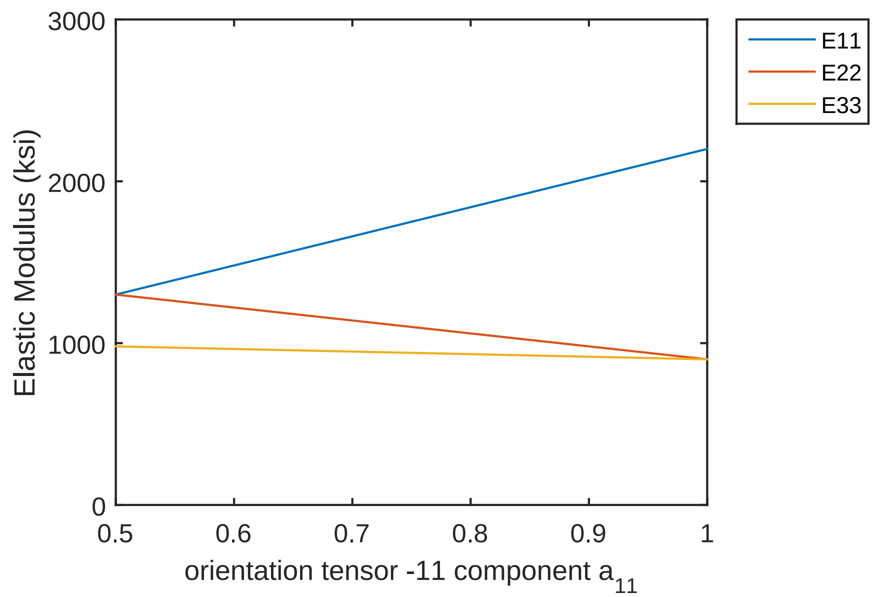

Figure 1.3: An example of elastic moduli as a function of the fiber orientation. Predicted values for Nylon 6/6 with 20% by volume of glass fibers with $L/D = 50$. Fiber orientation is planar, and varies from random ($a_{11} = 0.5$) in the 1-2 plane to aligned in the 1-direction ($a_{11} = 1$). (Reproduced with permission: Tucker and Advani, 1994. [2])

the experimental observations by Shaqfeh and Fredrickson [12]. Koch and Shaqfeh [13] calculated the average rotation rate of fibers in a linear shear flow, both in dilute and semi-dilute regimes, concluding that Jeffery's theory continues to provide a good approximation to the fiber rotation rate in the semi-dilute regime. In the same year, they developed a diagrammatic expansion to estimate the deviation from Jeffery orbit due to the hydrodynamic interaction [14].

Doi and Edwards [15, 16] investigated the "entanglement" dynamics between the polymer molecules with rotational diffusion coefficient D_r in a semiconcentrated solution, where polymer molecules are treated as "rods". Folgar and Tucker [17] assumed that the diffusivity is proportional to the shear rate, and modeled the fiber-fiber interactions as random collisions with an interaction coefficient C_I analogous to Brownian rotation diffusion. In this work, C_I was determined by fitting numerical results to the steady state orientation distribution function in shear flow, and was treated as a constant for a given suspension. The predicted C_I was then shown to result in a faster alignment than experimental observations. Their experimental results show that, for nylon and polyester fibers suspended in silicone oil under simple shear flow, steady state interaction coefficient C_I increases as the fiber concentration goes up. Another way to determine C_I is, instead of by fitting numerical results to the distribution function, by fitting the results to the orientation tensor components. Bay [18] used this method and generated a fitted equation from extensive empirical results. His work shows a different trend than Folgar and Tucker's result, which was suspected to be caused by fiber length distribution or other complex matrix rheology effect. Ma et al. developed a generalized orientation model for describing both steady shear and linear viscoelasticity data [19].

Advani and Tucker [20] propose to use tensors to describe the orientation state of fibers more concisely, freeing the representation from any assumptions about the shape of the probability distribution function. This system, however, requires a suitable closure approximation for accurate orientation predictions. Ranganathan and Advani considered the orientational clustering and proposed a statistical methods to characterize this phenomenon [21]. Cheng et al. describes the assembly process of vorticity-aligned hard-sphere colloidal strings in a simple shear flow [22].

Advani and Tucker tested several approximations and suggested a hybrid closure approximation [23]. Several other approximations were developed and tested [24, 25, 26, 27, 28, 29, 30].

Numerical simulations provide data under conditions inaccessible by experimentation. Ranganathan and Advani [31] proposed a variable interaction coefficient dependent on the inter-fiber spacing. Yamane et al. [32] developed a method to simulate the fiber motion in shear flow, with short-range interactions modeled by lubrication forces between neighboring fibers. Fan et al. [33] argues that the long-range hydrodynamic interactions may not be negligible in semi-concentrated suspensions, and revised this numerical simulation to incorporate both short- and long-range interactions, neglecting Brownian motion. They assumed an anisotropic diffusivity $\boldsymbol{C}$, and used the average of its diagonal components to be C_I. Phan-Thien et al. [34] reported another empirical equation for C_I using this method. Some other researchers have also embraced the idea of an anisotropic interaction coefficient [35, 36, 37].

1.3 Objectives and Approach

The extensive use of circular-particle-loaded in fiber composites is often to improve the compressive strength and to improve the toughening of the matrix. The objective of this work is to explore how the presence of circular particles changes the hydrodynamics of a fiber suspension, and how it can affect the fiber alignment in a Newtonian matrix undergoing a simple shear flow.

The approach followed to understand the fiber motion in the presence of circular particles is as follows:

- adapt the direct simulation method to simulate the hydrodynamics of a circular-particle loaded fiber suspension in a simple shear flow;
- observe the interactions between fibers and circular particles;
- calculate the steady-state interaction coefficient C_I for neat fiber suspension system and fiber-and-particle hybrid suspension system;
- compare the results with pre-existing models;
- compare the results to see the effects of the presence of circular particles in the system.

The direct bi-period simulation method has been successfully implemented to simulate circular-particle suspensions in both Newtonian and viscoelastic fluid [38, 39] and elliptical fiber suspensions [40]. Combining the concept of the bi-periodic domain with the mortar element methods[1], these researchers implemented a standard velocity-pressure formulation of a fictitious-domain finite-element method. Collision was avoided by reducing the time step when the suspension is not too concentrated, so no collision strategy was developed to the best of my knowledge. But, to simulate the non-dilute

[1] a type of discretization method where the interface between subdomains doesn't dictate the mesh boundary discretization. The quality of the solution is enforced by Lagrange multipliers [41, 42, 43].

short-fiber suspensions, a reasonable collision strategy must first be developed for situations where fibers rotate and get too close to each other and even when they collide.

This simulation method fully describes the motion of not only the fiber, but the flow as well. At each time step, the transverse and rotational velocity and displacement of each fiber is calculated and used as the starting point of the next step. The direction vector $\boldsymbol{p}$ of each fiber is then used to calculate the time evolution of the orientation state of the fibers for further analysis.

We will conduct the simulations for fiber suspensions with aspect ratio larger than 10, investigate the role of the concentrations of the fiber and the particle in the rheological behavior of the suspensions, and conclude whether the original fiber orientation will remain the same when circular particles are present in the same simple shear flow.

1.4 Thesis Overview

The goal of this work is to study the orientation of the force-free torque-free fibers suspended in a circular-particle-loaded suspension undergoing a simple shear flow in a Newtonian matrix. Chapter 2 lays out the fundamental theories and models that will be used to describe, characterize or quantify the the rheological properties of a circular-particle-loaded fiber system. Chapter 3 elaborates on the numerical implementation of the system of interest, proposes a specialized collision strategy to address the collision issues between solid bodies during the simulations, and discusses the choice of some simulation parameters such as the number of collocation points along the fiber surface. Chapter 4 presents the simulation approach to compare the diffusivity between fiber suspensions with and without circular particles, reports the simulation results of these two systems, and discusses the findings. Chapter 5 looks back on what is accomplished through this work and provides possible path forwards.

Chapter 2

THEORY

2.1 Definition of Concentrations of Fiber Suspensions

A suspension of uniform, cylindrical rods is characterized by the fiber volume fraction c, the fiber number density n, and the fiber aspect ratio $ar = L/D$, where L is the fiber length and D is the fiber diameter.

Dilute suspension

$$c \ll \frac{1}{ar^2} \quad \text{or} \quad n \ll \frac{1}{L^3} \tag{2.1}$$

Semi-concentrated/semi-dilute suspension

$$\frac{1}{ar^2} < c < \frac{1}{ar} \quad \text{or} \quad \frac{1}{L^3} < n < \frac{1}{L^2 D} \tag{2.2}$$

Concentrated suspension

$$c > \frac{1}{ar} \quad \text{or} \quad n > \frac{1}{L^2 D} \tag{2.3}$$

2.2 Fiber Orientation

2.2.1 Orientation of a single fiber

Suppose that each fiber is an axisymmetric particle, the orientation of it can be described by angle ϕ, which is the angle from x axis to the major axis of the fiber,

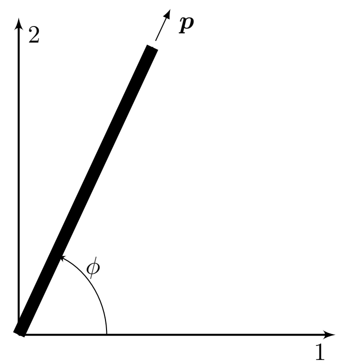

Figure 2.1: Definition of $\boldsymbol{p}$, ϕ, and directions for a fiber in a 2-dimensional system.

or a unit vector $\boldsymbol{p}$, and the location of it by (x, y). The components of $\boldsymbol{p}$ on a planar system (p_1, p_2) can then be described by

$$
\begin{aligned}
p_1 &= \cos\phi \\
p_2 &= \sin\phi
\end{aligned}
\tag{2.4}
$$

where $\phi \in (-\frac{\pi}{2}, \frac{\pi}{2})$ Due to the arbitrary nature of the choice of direction for the particle, any description of its orientation must remain the same if such substitution is made:

$$\phi \rightarrow \phi + \pi \tag{2.5}$$

or

$$\boldsymbol{p} \rightarrow -\boldsymbol{p} \tag{2.6}$$

2.2.2 Orientation distribution of many fibers

Distribution function

To describe planar fiber orientations in planar, one can assume that fibers are distributed uniformly in terms of concentration, while the orientation of those fibers may not be uniform. In this case, the state of orientation at a certain time is described by the *orientation distribution function* $\psi(\phi;t)$, it's defined such that the probability of a fiber with an orientation between ϕ_1 and ϕ_2 is

$$P(\phi_1 < \phi < \phi_2; t) = \int_{\phi_1}^{\phi_2} \psi(\phi;t)\,\mathrm{d}\phi \tag{2.7}$$

where ψ has the following properties:

$$\psi(\phi) = \psi(\phi+\pi) \quad \text{or} \quad \psi(\boldsymbol{p}) = \psi(-\boldsymbol{p}) \tag{2.8}$$

$$\int_{-\frac{\pi}{2}}^{\frac{\pi}{2}} \psi(\phi)\,\mathrm{d}\phi = \int \psi(\boldsymbol{p})\,\mathrm{d}\boldsymbol{p} = 1 \tag{2.9}$$

Continuity equation

One can define the angular velocity $\dot{\phi}$

$$\frac{\partial}{\partial t}\big[\psi(\phi)\,\delta\phi\big] = \psi(\phi)\,\dot{\phi}(\phi) - \psi(\phi+\delta\phi)\,\dot{\phi}(\phi+\delta\phi) \tag{2.10}$$

then, as $\delta\phi \to 0$,

$$\frac{\partial \psi}{\partial t} = -\frac{\partial}{\partial \phi}(\psi\dot{\phi}) \tag{2.11}$$

is known as *the continuity equation*.

For non-homogeneous case, i.e., ψ is dependent on location, hence the convective equation can be expressed as

$$\frac{\mathrm{D}\psi}{\mathrm{D}t} = -\frac{\partial}{\partial \phi}(\psi\dot{\phi}) = \frac{\partial \psi}{\partial t} + u\frac{\partial \psi}{\partial x} + v\frac{\partial \psi}{\partial y} \tag{2.12}$$

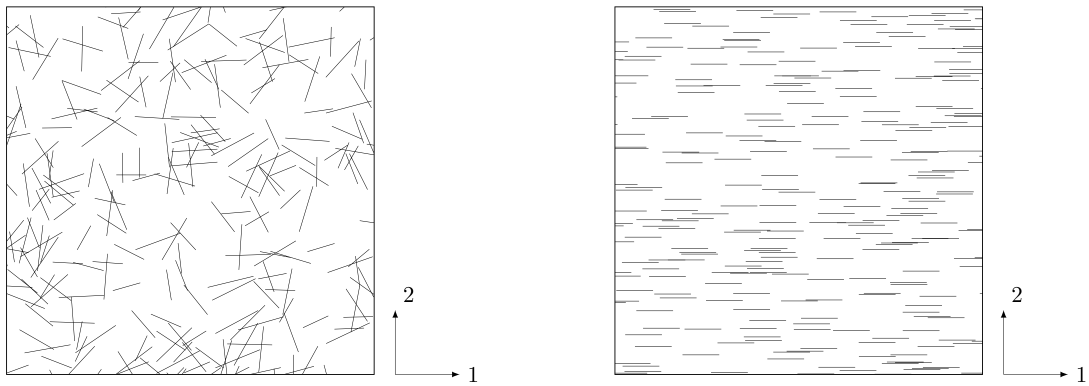

(a) $a_{11} = 0.5,\ a_{22} = 0.5,\ a_{12} = 0.$ (b) $a_{11} = 1,\ a_{22} = 0,\ a_{12} = 0.$

Figure 2.2: Examples of different orientation states. (a) Random in the 1-2 plane. (b) Aligned in the 1-direction

Orientation tensors

Let B represent an quantity that can be associated with a single fiber, and B^k is the value of B for the kth fiber. The *local volume average* of B, denoted by $\langle B\rangle$, is defined as

$$\langle B\rangle = \frac{1}{N}\sum_{k=1}^{N} B^k \tag{2.13}$$

Defining the 2nd-order orientation tensor $\boldsymbol{A}$ and 4th-order orientation tensor ${}^4\boldsymbol{A}$

$$\boldsymbol{A} = \oint \boldsymbol{pp}\psi(\boldsymbol{p})d\boldsymbol{p} = \langle \boldsymbol{pp}\rangle \tag{2.14}$$

$${}^4\boldsymbol{A} = \oint \boldsymbol{pppp}\psi(\boldsymbol{p})d\boldsymbol{p} = \langle \boldsymbol{pppp}\rangle \tag{2.15}$$

Figure 2.2 shows two distinct fiber orientation states, and their orientation tensor component values.

As $\boldsymbol{p}$ has unit length, it's easy to draw the following conclusions:

$$a_{ij} = a_{ji} \tag{2.16}$$

$$a_{ii} = 1 \tag{2.17}$$

$$a_{ij} = a_{ijkk} \tag{2.18}$$

2.3 Jeffery's Orbit and Rotary Diffusivity

2.3.1 Jeffery's orbit

Consider the motion of fibers in a flowing fluid. The classical analysis by Jeffery treats a single, rigid particle in an infinite body of Newtonian fluid. The unperturbed fluid velocity is assumed to be a linear function of position, and inertia and body forces are assumed to be negligible. Assuming arbitrary translation and rotation of an ellipsoidal particle, he developed analytical solutions for the velocity and pressure fields and derived the total force and moment exerted by the fluid on the particle. The particle motion was then solved by requiring the net force and net moment on the particle both to be zero.

Jeffery's solution shows that in a planar flow, the centroid of the particle translates with the unperturbed fluid velocity at that point, with its rotational motion written as an expression for the time derivative of the orientation vector $\boldsymbol{p}$,

$$\dot{p}_i = -\frac{1}{2}\omega_{ij}p_j + \frac{1}{2}\lambda(\dot{\gamma}_{ij}p_j - \dot{\gamma}_{kl}p_k p_l p_i) \tag{2.19}$$

where $\dot{\gamma}_{ij}$ and ω_{ij} are the rate-of-deformation and vorticity tensors respectively, given by

$$\dot{\gamma}_{ij} = \frac{\partial v_j}{\partial x_i} + \frac{\partial v_i}{\partial x_j} \tag{2.20}$$

$$\omega_{ij} = \frac{\partial v_j}{\partial x_i} - \frac{\partial v_i}{\partial x_j} \tag{2.21}$$

where v_i represents the unperturbed velocity of the fluid.

λ is a constant that depends on the particle shape. For ellipsoids of revolution where the length of symmetry axis is a and the length of the other two axes is b, the factor is

$$\lambda = \frac{(a/b)^2 - 1}{(a/b)^2 + 1} \tag{2.22}$$

For a sphere, $\lambda = 0$; for a slender particle,i.e.,$(a/b) \to \infty$, $\lambda \to 1$.

Jeffery's orbit in simple shear flow

Jeffery's equation predicts that a single particle in a simple shear flow will undergo a periodic rotation. In a flow field with shear rate $\dot{\gamma}$, and

$$v_1 = \dot{\gamma} x_2, \quad v_2 = v_3 = 0 \tag{2.23}$$

the fiber motion will then be

$$\tan\theta = \frac{C r_e}{\sqrt{\cos^2\phi + {r_e}^2 \sin^2\phi}} \tag{2.24}$$

$$\cot\phi = r_e \tan\left(\frac{2\pi t}{T} + \kappa\right) \tag{2.25}$$

where the period of rotation T is

$$T = \frac{2\pi}{\dot{\gamma}}\left(r_e + \frac{1}{r_e}\right) \tag{2.26}$$

where r_e is the effective value of (a/b), called *the equivalent ellipsoidal axis ratio*. *The Jeffery's orbit constant* C and the phase κ are determined by the initial orientation of the particle. If the motion of the particle is marked out in $\theta - \phi$ space, the particle will continually retrace the same path, and these motions are called *the Jeffery orbits*.

2.3.2 Rotary diffusivity

In simple shear flow, the orientation distribution achieves a steady state after a short time, with no oscillation or any periodicity. Current models that include an interaction effect are closely related to *the theory of rotary Brownian motion*. All particles in a suspension experience small, randomly-oriented forces as they collide with the solvent molecules. If the particles are extremely small, comparable to some colloidal particles or polymer molecules in solution, then these random motions are significant. These effects, called rotary Brownian motion on fiber orientation are modeled by adding a rotary diffusion term to the time evolution of the probability distribution function $\psi(\phi)$. In our case, the related "diffusion flux" $\psi\dot{\phi}$ is proportional to the gradient $\frac{\partial \psi}{\partial \phi}$, so the continuity equation 2.11 in planar flows is modified to be

$$\frac{\partial \psi}{\partial t} = -\frac{\partial}{\partial \phi}(\psi\dot{\phi}) + D_r \frac{\partial^2 \psi}{\partial \phi^2} \tag{2.27}$$

where $\frac{\partial}{\partial \phi}$ and $\frac{\partial^2}{\partial \phi^2}$ represent the gradient and Laplacian operators on the surface of a unit sphere, and D_r is the rotary diffusivity, a material property with units of (1/time), depending on the size of the particles and the temperature and viscosity of the suspending fluid.

When there's no deformation to drive the fiber motion, then $\dot{\phi} = 0$, the diffusion term therefore reduces the gradients in ψ, resulting in random orientation. When the suspension is deforming, then this term tends to resist the alignment caused by $\dot{\phi}$ term.

Although the fibers in practical composites are too large to experience significant Brownian motion, equation 2.27 exhibits many of the same qualitative features as non-dilute suspensions when D_r is small. Folgar and Tucker proposed adapting 2.27 by using $\lambda = 1$ in Jeffery's equation and setting

$$D_r = C_I \dot{\gamma} \tag{2.28}$$

where C_I, called the *interaction coefficient*, is an empirical material constant, and $\dot{\gamma}$ is the scalar magnitude of the rate-of-deformation tensor $\dot{\boldsymbol{\gamma}}$,

$$\dot{\gamma} = \sqrt{\frac{1}{2}\dot{\gamma}_{ij}\dot{\gamma}_{ji}} = \sqrt{2(\frac{\partial u}{\partial x})^2 + (\frac{\partial u}{\partial y} + \frac{\partial v}{\partial x})^2 + 2(\frac{\partial v}{\partial y})^2} \tag{2.29}$$

For planar flow and orientation, Folgar and Tucker's model reduces to

$$\dot{\phi} = -\frac{C_I \dot{\gamma}}{\psi}\frac{\partial \psi}{\partial \phi} - \sin\phi\cos\phi\,\frac{\partial u}{\partial x} - \sin^2\phi\,\frac{\partial u}{\partial y} + \cos^2\phi\,\frac{\partial v}{\partial x} + \sin\phi\cos\phi\,\frac{\partial v}{\partial y} \tag{2.30}$$

Combine it with equation 2.11,

$$\frac{\partial \psi}{\partial t} = C_I \dot{\gamma}\,\frac{\partial^2 \psi}{\partial \phi^2} + \frac{\partial}{\partial \phi}\big[\psi\,\big(\sin\phi\cos\phi\,\frac{\partial u}{\partial x} + \sin^2\phi\,\frac{\partial u}{\partial y} - \cos^2\phi\,\frac{\partial v}{\partial x} - \sin\phi\cos\phi\,\frac{\partial v}{\partial y})\big] \tag{2.31}$$

2.4 Tensor Equations

Substituting Eq. 2.27 with Eq. 2.14 and 2.15, and using Jeffery's equation 2.19, gives

$$\frac{\mathrm{D}a_{ij}}{\mathrm{D}t} + \frac{1}{2}\big(\omega_{ik}a_{kj} - a_{ik}\omega_{kj}\big) = \frac{1}{2}\lambda\big(\dot{\gamma}_{ik}a_{kj} + a_{ik}\dot{\gamma}_{kj} - 2\dot{\gamma}_{kl}a_{ijkl}\big) + 2C_I\dot{\gamma}\big(\delta_{ij} - \alpha a_{ij}\big) \quad (2.32)$$

whose left-hand side represents the Jaumann derivative of a_{ij}, and α equals 3 for three-dimensional orientation and 2 for planar orientation.

Using orientation tensors, though compact and computationally efficient, has its own drawbacks—that the 4th-order tensor a_{ijkl} appears in the governing equation for a_{ij} and thus causes a closure problem, which can only be solved by approximating the unknown moments in terms of the known moments.

To do this, the simplest closure—quadratic closure is given by

$$a_{ijkl} \approx a_{ij}a_{kl} \quad (2.33)$$

which is exact for fully-aligned fibers.

Advani and Tucker show that better steady-state results are obtained with *hybrid closure approximation*, for three-dimensional orientation,

$$\begin{aligned} a_{ijkl} \approx\ & f\big(a_{ij}a_{kl}\big) \\ & +(1-f)\big[-\frac{1}{35}\big(\delta_{ij}\delta_{kl} + \delta_{ik}\delta_{jl} + \delta_{il}\delta_{jk}\big) + \\ & \frac{1}{7}\big(a_{ij}\delta_{kl} + a_{ik}\delta_{jl} + a_{il}\delta_{jk} + a_{kl}\delta_{ij} + a_{jl}\delta_{ik} + a_{jk}\delta_{il}\big)\big] \end{aligned} \quad (2.34)$$

while for planar orientation,

$$
\begin{aligned}
a_{ijkl} \approx\ & f\big(a_{ij}a_{kl}\big) \\
& +(1-f)\big[-\frac{1}{24}\big(\delta_{ij}\delta_{kl}+\delta_{ik}\delta_{jl}+\delta_{il}\delta_{jk}\big)+ \\
& \frac{1}{6}\big(a_{ij}\delta_{kl}+a_{ik}\delta_{jl}+a_{il}\delta_{jk}+a_{kl}\delta_{ij}+a_{jl}\delta_{ik}+a_{jk}\delta_{il}\big)\big]
\end{aligned}
\tag{2.35}
$$

where f is a scalar measure of orientation,

$$
f = A a_{ij} a_{ji} - B \tag{2.36}
$$

where, for three-dimensional orientation,

$$
\begin{aligned}
A &= \frac{3}{2} \\
B &= \frac{1}{2}
\end{aligned}
\tag{2.37}
$$

and for planar orientation,

$$
\begin{aligned}
A &= 2 \\
B &= 1
\end{aligned}
\tag{2.38}
$$

There have been other closure approximations proposed which are more accurate. Verleye and Dupret [24]; and Dupret and Verleye [25] developed *natural closure*. Cintra and Tucker proposed *Orthotropic Closure* (ORT) [26]. Chung and Kwon proposed *Invariant-Based Optimal Fitting closure* (IBOF) [27], which is considered as a hybrid of the natural closure and the ORT closure. The simulations presented here provide the orientation of all fibers so the fiber orientation distribution and orientation can be directly obtained and closure approximations are not needed.

2.5 Fiber Interaction Coefficient C_I

The four components of C_I being calculated from the simulations can be derived from equation Eq. 2.32 (see Appendix A for detailed derivation process). As Eq. 2.39 shows, the four C_I components are actually two sets, as $C_{I_{12}} = C_{I_{21}}$, and $C_{I_{11}} = C_{I_{22}}$.

In this thesis, we use only $C_{I_{11}}$ to represent C_I. $C_{I_{11}}$ and $C_{I_{12}}$ are functions of a_{11} and a_{12} (and other variables). Because a_{11} and a_{12} appear in their denominators, this dependence carries over to all their derivatives. By observing the Eq. 2.39, we know that, when $a_{11} \in [0.65, 1]$ and $|a_{12}| \in [0, 0.2]$, $C_{I_{12}}$ can easily be subject to a deviation significantly greater than $C_{I_{11}}$'s — this is confirmed by preliminary numerical results, and unfortunately those are exactly the ranges of a_{11} and a_{12} when the fiber orientation stabilizes. So, we use $C_{I_{11}}$ as the C_I instead of $C_{I_{12}}$, as it's more consistent in values and easier to analyze (see Appendix B for more discussions).

$$\begin{aligned}
C_{I_{11}} &= \frac{\dfrac{\partial a_{11}}{\partial t} - (1+\lambda)\dot{\gamma} a_{12} + 2\lambda\dot{\gamma} a_{1112}}{2\dot{\gamma}(1-2a_{11})} \\
C_{I_{22}} &= \frac{\dfrac{\partial a_{11}}{\partial t} - (1+\lambda)\dot{\gamma} a_{12} + 2\lambda\dot{\gamma} a_{1112}}{2\dot{\gamma}(1-2a_{11})} \\
C_{I_{12}} &= \frac{-\dfrac{\partial a_{12}}{\partial t} - \dfrac{\dot{\gamma}}{2}(2a_{11}-\lambda-1) - 2\lambda\dot{\gamma} a_{1122}}{4\dot{\gamma} a_{12}} \\
C_{I_{21}} &= \frac{-\dfrac{\partial a_{12}}{\partial t} - \dfrac{\dot{\gamma}}{2}(2a_{11}-\lambda-1) - 2\lambda\dot{\gamma} a_{1122}}{4\dot{\gamma} a_{12}}
\end{aligned} \tag{2.39}$$

There are several models used to describe C_I. Bay's empirical results suggest a fitting curve for C_I as a function of $\dfrac{\phi_f L}{D}$ [18]

$$C_I = 0.0184\exp(-0.7148\phi_f\frac{L}{D}) \qquad , \tag{2.40}$$

Ranganathan and Advani [31] propose a theoretical model using Doi-Edwards theory as

$$C_I = \frac{K}{a_c/L} \qquad , \tag{2.41}$$

where K is a proportionality constant and a_c is the average inter-fiber spacing, which itself is dependent on the fiber orientation states. Fan et al. [33] developed another exponential equation to model the relationships between C_I and the fiber aspect ratio and concentration using their simulation results

$$C_I = 0.03\big[1 - \exp(-0.224\phi_f\frac{L}{D})\big] \qquad . \tag{2.42}$$

There are also some anisotropic diffusivity models developed [35] [36] [37].

2.6 Shear Stress

Following the work of Dinh and Armstrong, we get the following stress expression,

$$\sigma_{ij} = -p\delta_{ij} + \eta\dot{\gamma}_{ij} + \tau_{f\,ij} \tag{2.43}$$

where

$$\tau_{f\,ij} = \frac{1}{2}\eta N_p\ a_{ijkl}\dot{\gamma}_{kl} + \beta D_r(a_{ij} - \frac{1}{3}\delta_{ij}) \tag{2.44}$$

whose second term on the right hand side is negligible in steady shear case, and where N_p is a scalar parameter that depends on the fiber concentration as well as the aspect ratio of fibers.

Then the expression for shear stress becomes

$$\sigma_{ij} = -p\delta_{ij} + \eta\dot{\gamma}_{ij} + \frac{1}{2}\eta N_p a_{ijkl}\dot{\gamma}_{kl} \tag{2.45}$$

Chapter 3

DIRECT SIMULATION METHOD

A finite element scheme for direct simulations of inertialess particle suspensions in simple shear flows of a Newtonian fluid [38] was used. The whole domain was discretized with bi-quadratic interpolations of the velocity and linear discontinuous interpolations of the pressure. Two different kinds of Lagrangian multipliers are used, one for the sliding bi-periodic constraints and the other one for the rigid-ring problem, where the movement of a rigid body (an elliptical fiber or a circular particle) is represented by collocation points along its circumference, forming a “rigid-ring”. The bulk stress can be expressed by simple boundary integrals of the multipliers along domain boundaries and along particle boundaries.

3.1 Modeling

3.1.1 Problem definition

We consider flowing suspensions consisting of a large number of non-Brownian circular disk particles and elliptical fibers in a Newtonian fluid undergoing a simple shear flow. The rigid body motions of the fibers are particles that are force-free, torque-free, and inertialess.

3.1.2 Computation domain

In order to observe the complex particle/fiber motions and hydrodynamic interactions, the bi-periodic domain is introduced. This bi-period domain may transform a

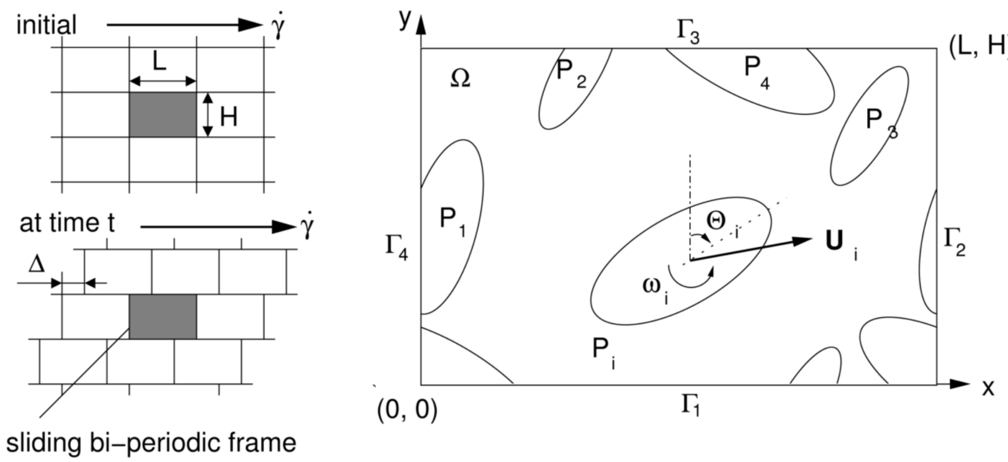

Figure 3.1: Sliding bi-periodic frames in a simple shear flow (*left*). A sliding bi-periodic frame is the computational domain and a possible fiber configuration inside the domain (*right*). Positive direction of rotation and angular velocity is counterclockwise. (Reproduced with permission: Chung et al., 2005. [40])

suspension in an unbounded domain with an infinite number of particles/fibers into a simple shear problem in a unit cell, giving a peek at the behavior of the suspension. The rigid body motions of the fibers and particles are described through rigid-ring constraints which are implemented by Lagrangian multipliers only on the particle boundary.

Figure 3.1 shows sliding bi-periodic frames and a possible fiber configuration in a single frame. At an arbitrary instance, say $t = 0$, an unbounded domain of interest can be regularly divided into an infinite number of frames with width L and height H. Each frame within this unbounded domain will translate along the shear direction at its own average velocity of the flow inside the frame. Rows of the frames slide relatively to one another by an amount Δ. Δ between upper and lower frames is given by

$$\Delta = \dot{\gamma} H t \tag{3.1}$$

where $\dot{\gamma}$ is the shear rate, and t is the elapsed time.

The sliding frame is an inertial frame of reference, which translates at a constant velocity. The velocity is determined by the shear rate and a representative vertical position based on an arbitrary global reference coordinate in order to represent a simple shear problem. The sliding frame is bi-periodic, which means particles/fibers crossing the left frame boundary should re-appear on the right boundary, particles/fibers crossing the upper boundary should re-appear on the lower boundary, and vice versa. The bi-periodicity is time-dependent. The periodicity between upper and lower boundaries is determined by the amount of slide Δ, which itself is a function of time.

A sliding bi-periodic frame, denoted by Ω, is the computational domain of this work. It consists of: four boundaries of the frame Γ_i, (i=1-4), particles/fibers are denoted by $P_i, (i = 1, 2, ..., N)$ (N is the number of particles/fibers in a single frame). The Cartesian coordinates x and y are chosen as parallel and normal to the shear flow direction respectively.

The i-th particle/fiber P_i has the following properties to denote:

- the particle/fiber center $\boldsymbol{X}_i = (X_i, Y_i)$
- the translation velocity $\boldsymbol{U}_i = (U_i, V_i)$
- the angular velocity $\boldsymbol{\omega}_i = \omega_i \boldsymbol{k}$
- the angular rotation $\boldsymbol{\Theta}_i = \Theta_i \boldsymbol{k}$

where $\boldsymbol{k}$ is the unit vector in the direction normal to and out of the plane.

3.1.3 Governing equations

Here, we present the governing equations in a strong form for suspensions of two-dimensional particles/fibers in a Newtonian fluid, neglecting inertia for both fluid and particles/fibers.

The equations for systems consisting of only non-boundary-crossing particles/fibers are presented first.

Fluid domain

momentum balance

$$\boldsymbol{\nabla} \cdot \boldsymbol{\sigma} = 0 \qquad \text{in } \Omega \backslash P(t) \tag{3.2}$$

mass balance

$$\boldsymbol{\nabla} \cdot \boldsymbol{u} = 0 \qquad \text{in } \Omega \backslash P(t) \tag{3.3}$$

the constitutive relation

$$\boldsymbol{\sigma} = -p\boldsymbol{I} + 2\eta\boldsymbol{D} \qquad \text{in } \Omega \backslash P(t) \tag{3.4}$$

rigid body motion on the particle/fiber surface

$$\boldsymbol{u} = \boldsymbol{U_i} + \omega_i \times (\boldsymbol{x} - \boldsymbol{X_i}) \text{ on } \partial P_i(t) \quad \text{(i=1,…,N).} \tag{3.5}$$

where

$\boldsymbol{\sigma}$ is the stress tensor

$\boldsymbol{u}$ is the velocity vector

p is the pressure

$\boldsymbol{I}$ is the identity tensor

η is the viscosity

and $\boldsymbol{D}$ is the rate of deformation tensor

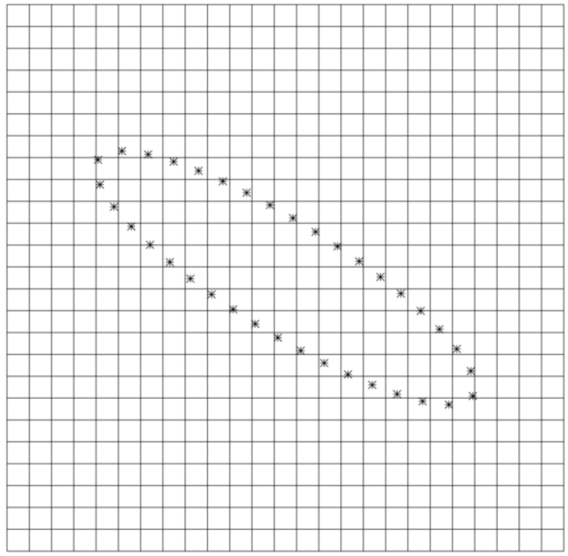

Figure 3.2: The fiber is described by evenly distributed collocation points along its boundary. The entire computational domain is described by a regular rectangular discretization. (Reproduced with permission: Chung et al., 2005. [40])

Rigid body domain

An alternative description for the fiber/particle domain is used here, called “rigid-ring description”. As shown in Figure 3.2, his method considers the particle/fiber as a rigid ring, which is filled with a fluid so that the rigid-body conditions are imposed on the particle boundary only. Discretization is therefore only needed along the particle/fiber boundary. It allows a systematic and respective treatment of boundary-crossing particles/fibers, but it’s only possible when inertia is negligible.

From the rigid-ring description, the governing equations for a region occupied by a particle P_i at a certain time t can be written as follows

momentum balance

$$\nabla \cdot \boldsymbol{\sigma} = 0 \qquad \text{in } P_i(t) \tag{3.6}$$

mass balance

$$\nabla \cdot \boldsymbol{u} = 0 \qquad \text{in } P_i(t) \tag{3.7}$$

the constitutive relation

$$\boldsymbol{\sigma} = -p\boldsymbol{I} + 2\eta\boldsymbol{D} \qquad \text{in } P_i(t) \tag{3.8}$$

rigid body motion on the particle/fiber surface

$$\boldsymbol{u} = \boldsymbol{U_i} + \omega_i \times (\boldsymbol{x} - \boldsymbol{X_i}) \text{ in } P_i(t) \tag{3.9}$$

In addition, the movement of the particles is given by the kinematic equations:

$$\frac{\mathrm{d}\boldsymbol{X}_i}{\mathrm{d}t} = \boldsymbol{U}_i \tag{3.10}$$

$$\frac{\mathrm{d}\boldsymbol{\Theta}_i}{\mathrm{d}t} = \boldsymbol{\omega}_i \tag{3.11}$$

Hydrodynamic interactions

In the absence of inertia and external forces or torques, the balance equations for the drag forces and torques on the boundary of P_i at time t are

$$\boldsymbol{F}_i = \int_{\partial P_i(t)} \boldsymbol{\sigma} \cdot \boldsymbol{n} \, \mathrm{d}s \qquad = 0 \tag{3.12}$$

$$\boldsymbol{T}_i = \int_{\partial P_i(t)} (\boldsymbol{x} - \boldsymbol{X}_i) \times (\boldsymbol{\sigma} \cdot \boldsymbol{n}) \, \mathrm{d}s \quad = 0 \tag{3.13}$$

Sliding bi-periodic frame constraints

For the horizontal periodicity between Γ_2 and Γ_4, the velocity continuity and force balance equations are:

$$\boldsymbol{u}(0,y) = \quad \boldsymbol{u}(L,y), \quad y \in [0,H] \tag{3.14}$$

$$\boldsymbol{t}(0,y) = -\,\boldsymbol{t}(L,y), \quad y \in [0,H] \tag{3.15}$$

where the vector $\boldsymbol{t}$ denotes the traction force on the boundary.

For the vertical periodicity between Γ_1 and Γ_3, the time-dependent velocity continuity and force balance equations are:

$$\boldsymbol{u}(x,H;t) = \quad \boldsymbol{u}(\{x-\dot{\gamma}Ht\}^*,0;t) + \boldsymbol{f}, \quad x \in [0,L) \tag{3.16}$$

$$\boldsymbol{t}(x,H;t) = -\,\boldsymbol{t}(\{x-\dot{\gamma}Ht\}^*,0;t) \qquad , \quad x \in [0,L) \tag{3.17}$$

where $\boldsymbol{f} = (\dot{\gamma}H, 0)$, and $\{\cdot\}^*$ denotes the modular function of L: e.g., $\{1.7L\}^* = 0.7L$ and $\{-1.7L\}^* = 0.3L$.

Boundary-crossing particles

We now consider fibers/particles that cross the computation domain boundaries Γ (Figure 3.1), where particles or parts of a particle are present outside the domain Ω. In this situation, such parts need to be relocated into the domain, and the velocity doesn't necessarily remain the same as those that do not cross the boundaries. The relocation proceeds in two steps: relocation of particle centers and relocation of particle boundaries. The relocated position of P_i, $\boldsymbol{x}_i' = (x_i', y_i')$, from the original position of

P_i, $\boldsymbol{x}_i = (x_i, y_i)$, is

$$\begin{aligned}
\boldsymbol{x}_i' &= (\{x_i - \dot{\gamma}Ht\}^*, \quad y_i - H), && \text{for } \boldsymbol{x}_i \in \Gamma_3 \\
\boldsymbol{x}_i' &= (\{x_i + \dot{\gamma}Ht\}^*, \quad y_i + H), && \text{for } \boldsymbol{x}_i \in \Gamma_1 \\
\boldsymbol{x}_i' &= (\{x_i\}^*, \quad y_i), && \text{for } \boldsymbol{x}_i \in \Gamma_2 \cup \Gamma_4
\end{aligned} \tag{3.18}$$

and the modified translational velocity component U of a particle is determined by the region where the original position is located:

$$\begin{aligned}
U' &= U - \dot{\gamma}H, && \text{for } \boldsymbol{x}_i \in \Gamma_3 \\
U' &= U + \dot{\gamma}H, && \text{for } \boldsymbol{x}_i \in \Gamma_1
\end{aligned} \tag{3.19}$$

Weak form

With the collision issues properly addressed, now we can move on to the weak form. The rigid-ring constraint in the combined velocity space is removed by enforcing it as a constraint equation in the weak form. Define Lagrangian multipliers

$$\boldsymbol{\lambda}^{\mathrm{h}} \in L^2(\Gamma_4) \tag{3.20}$$

$$\boldsymbol{\lambda}^{\mathrm{v}} \in L^2(\Gamma_3) \tag{3.21}$$

$$\boldsymbol{\lambda}^{\mathrm{p},i} \in L^2(\partial P_i(t)) \qquad (i = 1, ..., N) \tag{3.22}$$

to represent the traction on the computation domain boundary Γ_4, Γ_3 and on the particle surfaces $\partial P_i(t)$ respectively.

The weak form for the whole domain can then be written as

$$
\begin{aligned}
-\int_\Omega p\nabla\cdot\boldsymbol{v}\,\mathrm{d}A+\int_\Omega 2\eta\boldsymbol{D}(\boldsymbol{u}):\boldsymbol{D}(\boldsymbol{v})\,\mathrm{d}A+\sum_i^N\langle\boldsymbol{\lambda}^{\mathrm{p},i},\boldsymbol{v}-(\boldsymbol{V}_i+\boldsymbol{\chi}_i\times(\boldsymbol{x}-\boldsymbol{X}_i))\rangle_{\partial P_i}&\\
+\langle\boldsymbol{\lambda}^{\mathrm{v}},\boldsymbol{v}(x,H;t)-\boldsymbol{v}(\{x_i+\dot\gamma Ht\}^*,0;t)\rangle_{\Gamma_3}+\langle\boldsymbol{\lambda}^{\mathrm{h}},\boldsymbol{v}(0,y)-\boldsymbol{v}(L,y)\rangle_{\Gamma_4}=0 & \qquad (3.23)\\
\int_\Omega q\nabla\cdot\boldsymbol{u}\,\mathrm{d}A =&0 \qquad (3.24)\\
\langle\boldsymbol{\mu}^{\mathrm{p},i},\boldsymbol{u}-(\boldsymbol{U}_i+\boldsymbol{\omega}_i\times(\boldsymbol{x}-\boldsymbol{X}_i))\rangle_{\partial P_i} =&0 \qquad (3.25)\\
\langle\boldsymbol{\mu}^{\mathrm{h}},\boldsymbol{u}(0,y)-\boldsymbol{u}(L,y)\rangle_{\Gamma_4} =&0 \qquad (3.26)\\
\langle\boldsymbol{\mu}^{\mathrm{v}},\boldsymbol{u}(x,H;t)-\boldsymbol{u}(\{x-\dot\gamma Ht\}^*,0;t)\rangle_{\Gamma_3} =&\langle\boldsymbol{\mu}^{\mathrm{v}},\boldsymbol{f}\rangle_{\Gamma_3} \qquad (3.27)
\end{aligned}
$$

where the inner product $\langle\cdot,\cdot\rangle_{\Gamma_j}$ is the standard inner product in $L^2(\Gamma_j)$

$$\langle\boldsymbol{\mu},\boldsymbol{v}\rangle_{\Gamma_j} = \int_{\Gamma_j}\boldsymbol{\mu}\cdot\boldsymbol{v}\,\mathrm{d}s,$$

the forcing term $\boldsymbol{f}$ originates from the difference in the sliding velocities of the upper and the lower boundaries, and it is constant for giver $(\dot\gamma H)$. The weak form of the rigid-ring description (Eq. 3.25) is then approximated by point collocation by the particle boundaries

$$\langle\boldsymbol{\mu}^{\mathrm{p},i}(\boldsymbol{x}),\boldsymbol{u}(\boldsymbol{x})-(\boldsymbol{U}_i+\boldsymbol{\omega}_i\times(\boldsymbol{x}-\boldsymbol{X}_i))\rangle_{\partial P_i}\approx\sum_{k=1}^{M^i}\boldsymbol{\mu}_k^{\mathrm{p},i}\cdot[\boldsymbol{u}(\boldsymbol{x}_k)-(\boldsymbol{U}_i+\boldsymbol{\omega}_i\times(\boldsymbol{x}-\boldsymbol{X}_i))] \qquad (3.28)$$

where M^i,$\boldsymbol{x}_k$, and $\boldsymbol{u}(\boldsymbol{x}_k)$ are the number of collocation points on ∂P_i, the coordinate of the k-th collocation point on ∂P_i, and the collocated multiplier $\boldsymbol{\mu}_k^{\mathrm{p},i}$ at $\boldsymbol{x}_k$ respectively.

3.2 Collision Strategy

As reported by many researchers, the fibers tend to cluster under shear [21]. This issue is more pronounced in our non-dilute simulations as they are carried out in a 2-dimensional domain, where longer fibers do not have enough degree of freedom to avert collision by rotating to another plane. Although the domain inside the fiber are constrained to follow a rigid-body motion, it does not prevent the collocation points of another fiber from entering it (see Figure 3.2).

Finding an effective collision strategy is crucial. Glowinski et al. [44] proposed a collision strategy to apply to particulate flows. This strategy assumes a quadratic form of repulsive force between circular particles when the distance is closer than a designated safe distance ρ. It unfortunately doesn't adress fibers with aspect ratio larger than unity. Laure et al. [45] reported a collision strategy for cylindrical fibers in a 3-dimensional simulation. This method directly manipulates the position of each fiber further away from each other until all fibers are separated by a safe distance ρ. It is effective in theory, but it would not work well for our 2-dimensional domain as the packing won't allow for this kind of manipulation. Rezak [46] used an exponential formula for the repulsive force between flexible cylindrical fibers.

As there is no work on collision strategy between elliptical fibers proposed before, I propose an original collision strategy specifically to use for this case. A numerical algorithm was employed in this work [47] to gauge the minimum distance between two elliptical fibers, as no analytic solution is available. "Virtual rings" are constructed for fibers and circular particles that are crossing the computational boundaries (Figure 3.3) or closer to the boundary than the "safe distance".

As explained in Figure 3.4, the collision strategy takes effect in two parts:

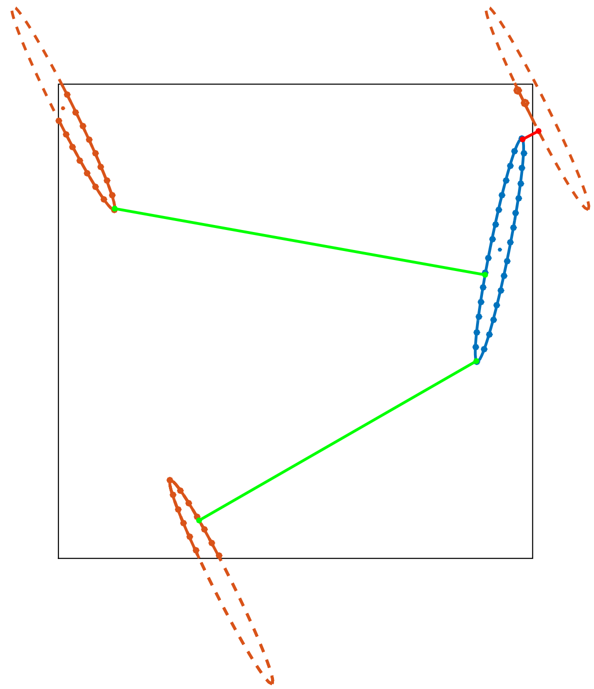

Figure 3.3: A diagram showing minimum distance calculation process and pre-collision detection between two fibers (*solid line*). Virtual rings (*dashed line*) are constructed for boundary-crossing fiber (*red*). 31 collocation points (CPs) uniformly distributed along the circumference of each fiber are marked with dots, number of CPs used the simulations are much greater. The red line between the blue fiber and one of the "virtual ring"s of the other showcases a near-collision situation, while green ones are in safe distances.

pre-collision and post-collision. Note that all the treatments are directly applied to the original fiber/particle instead of the "virtual rings", which are only constructed to determine the minimum distances.

3.2.1 Pre-collision treatments

The pre-collision strategy applies a force-pair to the nearest points along the surface of the two meeting fibers. This is achieved by adding $\boldsymbol{\lambda}^{\mathrm{p}}_{\mathrm{pre}}$ to the Lagrange multiplier $\boldsymbol{\lambda}^{\mathrm{p}}$ on the rigid body collocation points,

$$\boldsymbol{\lambda}^{\mathrm{p}}_{\mathrm{pre}_{ij}} = \begin{cases} 0 & , \qquad \|\boldsymbol{X}_i - \boldsymbol{X}_j\| > \rho \\ \epsilon_{\mathrm{rep1}} \dfrac{\boldsymbol{X}_i - \boldsymbol{X}_j}{\|\boldsymbol{X}_i - \boldsymbol{X}_j\|} \mathrm{e}^{-\epsilon_{\mathrm{rep2}}\|\boldsymbol{X}_i - \boldsymbol{X}_j\|} & , \qquad 0 < \|\boldsymbol{X}_i - \boldsymbol{X}_j\| \leq \rho \end{cases} \tag{3.29}$$

where ρ is the force range, $\boldsymbol{X}_i$ and $\boldsymbol{X}_j$ are the points along the surface of fiber$_i$ and fiber$_j$ respectively, ϵ_{rep1} and ϵ_{rep2} are repulsiveness parameters.

This will deliver a force to the point on each of the fiber where it's most closely approached. In most cases, the force will not coincide with the coordinates of the collocation points. In such cases, the treatment force $\boldsymbol{\lambda}^{\mathrm{p}}_{\mathrm{pre}_{ij}}$ should be split into a pair of forces and applied to the closest two collocation points available.

3.2.2 Post-collision treatments

The post-collision strategy, however, is more complicated. Because the finite-element scheme in use does not hard-code one fiber from another, so when they collide, i.e., one or more collocation points of one fiber travel into the ring encircled by the collocations points of another fiber, applying any form of force to the collision spot will be done to both of them, which will not separate them. Therefore, the following artificial forms of post-collision velocities are introduced to manage this situation.

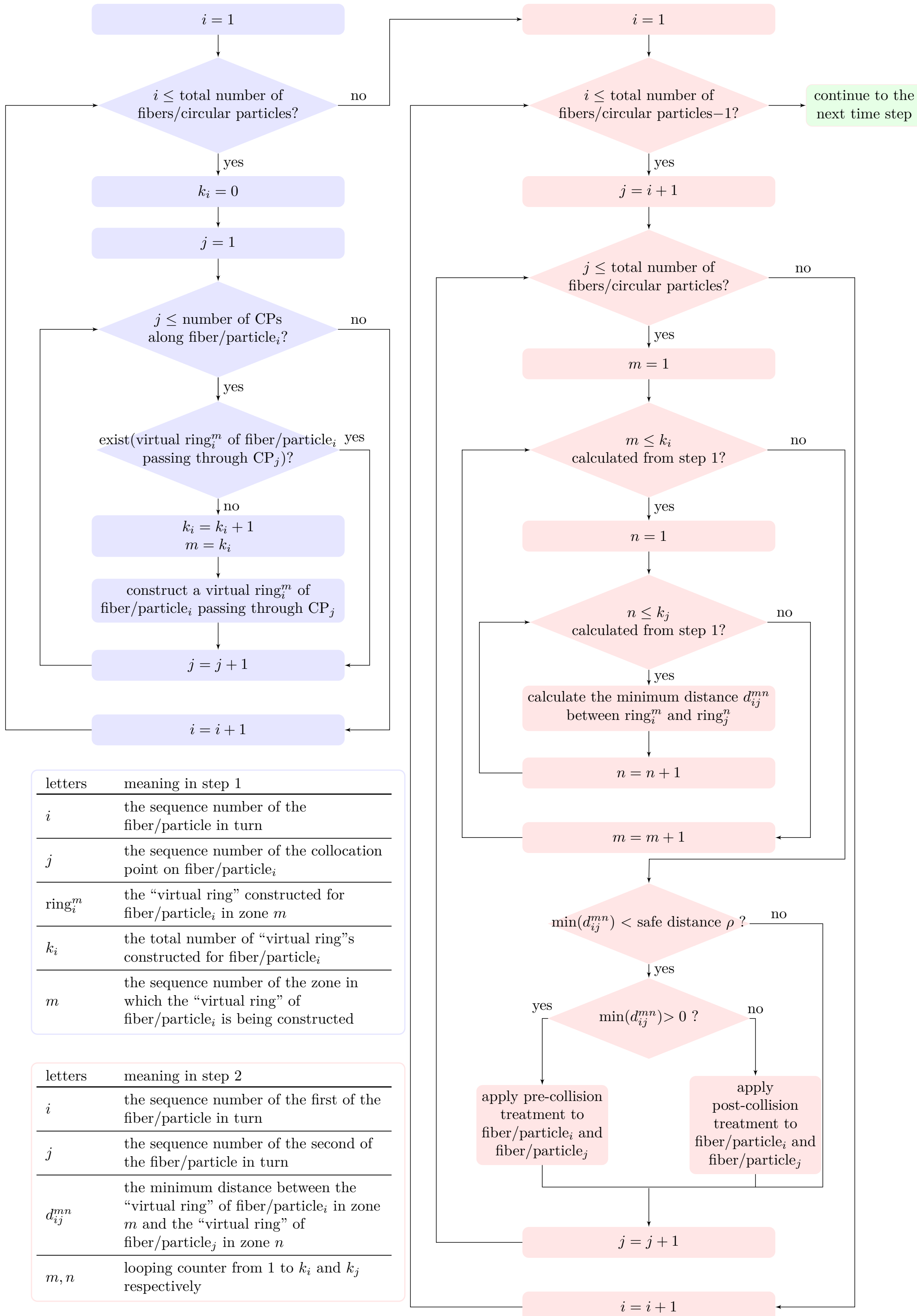

letters	meaning in step 1
i	the sequence number of the fiber/particle in turn
j	the sequence number of the collocation point on fiber/particle$_i$
ring$_i^m$	the "virtual ring" constructed for fiber/particle$_i$ in zone m
k_i	the total number of "virtual ring"s constructed for fiber/particle$_i$
m	the sequence number of the zone in which the "virtual ring" of fiber/particle$_i$ is being constructed

letters	meaning in step 2
i	the sequence number of the first of the fiber/particle in turn
j	the sequence number of the second of the fiber/particle in turn
d_{ij}^{mn}	the minimum distance between the "virtual ring" of fiber/particle$_i$ in zone m and the "virtual ring" of fiber/particle$_j$ in zone n
m, n	looping counter from 1 to k_i and k_j respectively

Figure 3.4: Implementation flowchart for pre- and post- collision between fibers and circular particles. "Virtual rings" are constructed in this process for boundary-crossing fibers and particles. The light blue items are of step 1, and the pink items are of step 2.

$$\boldsymbol{U}_{\text{post}_{ij}} = \epsilon_{\text{rep3}} \frac{\boldsymbol{X}_i^{\text{c}} - \boldsymbol{X}_j^{\text{c}}}{\left\|\boldsymbol{X}_i^{\text{c}} - \boldsymbol{X}_j^{\text{c}}\right\|} \, \mathrm{e}^{\epsilon_{\text{rep4}} \frac{\gamma_{ij}}{\pi}} \tag{3.30}$$

$$\boldsymbol{\Omega}_{\text{post}_{ij}} = (\text{ar}_i - 1) \sum_{k=1}^{2} \left(\boldsymbol{X}_k - \boldsymbol{X}_i^{\text{c}}\right) \times \left(\epsilon_{\text{rep5}} \, \mathrm{e}^{\epsilon_{\text{rep6}} \frac{\gamma_{ij}}{\pi}} \boldsymbol{n}_i^{\perp}\right) \tag{3.31}$$

where $\boldsymbol{U}_{\text{post}_{ij}}$ and $\boldsymbol{\Omega}_{\text{post}_{ij}}$ are the post-collision artificial linear/angular velocity exerted to fiber$_i$, ar$_i$ is the aspect ratio of fiber$_i$, $\boldsymbol{X}_i^{\text{c}}$ is the coordinates of the center of fiber$_i$, $\boldsymbol{X}_k$ $(k = 1, 2)$ are the coordinates of the intersection points on fiber$_i$, γ_{ij} is the angle between the eccentric anomalies of the intersection points of fiber$_i$, $\epsilon_{\text{rep3}-6}$ are repulsiveness parameters, and $\boldsymbol{n}_i^{\perp}$ is the unit vector perpendicular to the line connecting the two intersection points pointing towards fiber$_i$. Here we don't consider the case where fibers have more than two intersection points, as it should be prevented by the aforementioned regime.

The severity of the collision is measured by γ_{ij} — the deeper the fibers intersect into another, the stronger the artificial velocities the collision strategy will trigger. The resulted artificial linear velocity detach the fibers away along the connecting center line direction. And the resulting angular velocity (zero for the circular particles due to the ar$_i$ term) should move the fibers away from each other.

3.2.3 Collision strategy parameters

Many trials were performed to generate parameters with time during fiber/particle collision. The process to find the best parameters was analogous to gradient descent method, except that no function is available to characterize how well the parameters are preventing the fibers from colliding. Because the fibers seldom separate from each other once collision happens, I visually examine the extent of the fibers "tangling up" after a fixed period of simulation time. Take Eq. 3.30 for example. First, 3–5 values are chosen for ϵ_{rep3} and ϵ_{rep4}, run the simulations with all combinations of those values, decide which parameter the simulation is more sensitive to, say ϵ_{rep3}, narrow the range of ϵ_{rep3} to the ones where the simulations have less "tangled" fibers, repeat the steps for the other parameter(s) ϵ_{rep4}, then for ϵ_{rep3} again, repeat until an acceptable amount of collision is reached. Table 3.1 lists all the parameters used for the implementation of the proposed collision strategy.

Table 3.1: Parameters for collision strategy

ϵ_{rep1} [Pa]	ϵ_{rep2} [m^{-1}]	ϵ_{rep3} [ms^{-1}]	ϵ_{rep4} [1]	ϵ_{rep5} [m^{-1}s^{-1}]	ϵ_{rep6} [1]
1.0×10^{-2}	2.7×10^{2}	2.0×10^{1}	4.0×10^{0}	1.0×10^{-2}	6.0×10^{0}

Figure 3.5 plots the pre-collision force $\lambda^p_{\text{pre}_{ij}}$ applied to collocation points along the circumference of the fiber/particle P_i when the minimum distance of it from P_j is smaller than the designated safe distance ρ without touching. Figure 3.6 plots the post-collision translational velocity $\boldsymbol{U}_{\text{post}_{ij}}$ and angular velocity $\boldsymbol{\Omega}_{\text{post}_{ij}}$ applied to the center of the fiber/particle P_i after its collision with P_j.

Figure 3.7 gives an example of the proposed collision strategy. The column on the left shows the computational domain and fiber configuration at time $t = 0$ and $t = 20$ without the collision strategy, while the right with the strategy. Green dots along fiber surfaces denote the near-collision occurrences, where the pre-collision treatment force $\boldsymbol{\lambda}^{\text{p}}_{\text{pre}}$ ought to be applied. Green dots in the centers of the fibers denote occurrences, where the post-collision treatment velocities $\boldsymbol{U}_{\text{post}_{ij}}$ and $\boldsymbol{\Omega}_{\text{post}_{ij}}$ should be applied. It clearly shows that, (a) the collision is inevitable and a collision strategy is necessary, and (b) the effect of intersections amplifies over time, and the proposed

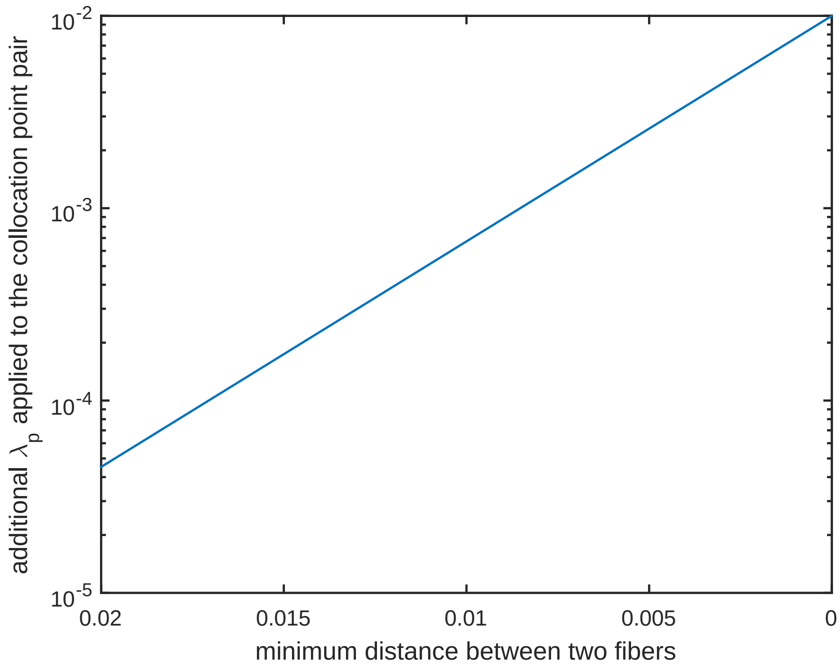

Figure 3.5: Pre-collision force $\lambda^p_{\text{pre}_{ij}}$ applied to collocation points along the circumference of the fiber/particle, $0 < \|\boldsymbol{X}_i - \boldsymbol{X}_j\| \leq \rho,\ \rho = 0.2$.

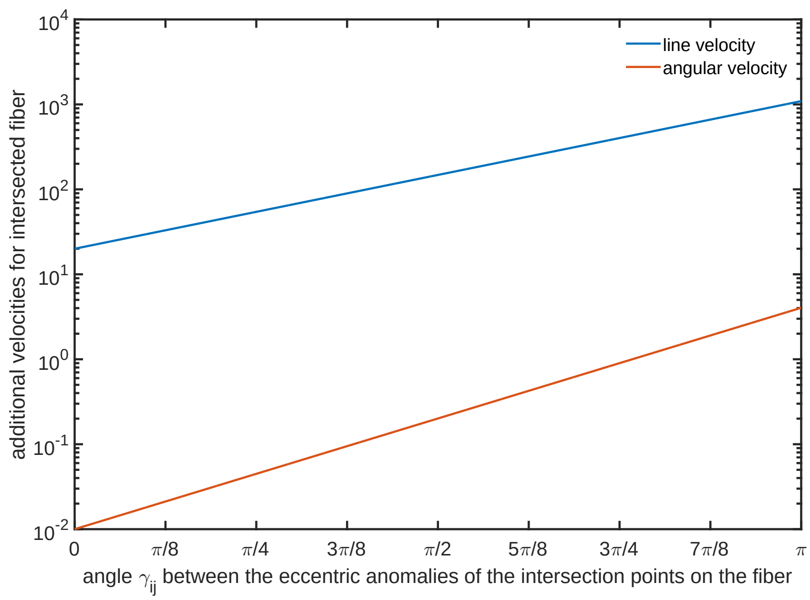

Figure 3.6: Post-collision velocities applied to the center of the fiber/particle

collision strategy significantly eliminates that.

3.3 Implementation

3.3.1 Discretization

Two discretization schemes are used in the simulations. A regular rectangular discretization with the bi-quadratic interpolation of the velocity and the linear discontinuous interpolation for the pressure is used. The $Q_2 - P_1^d$ element is illustrated in Figure 3.8, which satisfies the inf-sup condition[1].

3.3.2 Matrix equations

For each time step, the following matrix equation is solved for a given particle/fiber configuration:

$$\begin{bmatrix} K & G & 0 & P & H & V \\ G^T & 0 & 0 & 0 & 0 & 0 \\ 0 & 0 & 0 & R & 0 & 0 \\ P^T & 0 & R^T & 0 & 0 & 0 \\ H^T & 0 & 0 & 0 & 0 & 0 \\ V^T & 0 & 0 & 0 & 0 & 0 \end{bmatrix} \begin{bmatrix} \boldsymbol{u} \\ \tilde{p} \\ \tilde{\boldsymbol{U}} \\ \boldsymbol{\lambda}^p \\ \boldsymbol{\lambda}^h \\ \boldsymbol{\lambda}^v \end{bmatrix} = \begin{bmatrix} 0 \\ 0 \\ 0 \\ \tilde{\boldsymbol{f}}' \\ 0 \\ \tilde{\boldsymbol{f}} \end{bmatrix} \tag{3.32}$$

where $\tilde{p}$, $\tilde{\boldsymbol{U}}$, $\tilde{\boldsymbol{f}}$, $\tilde{\boldsymbol{f}}'$ are pressure variables, rigid-body motion variables, the forcing term due to the vertical sliding periodicity (Eq. 3.27), and the integral of the forcing term due to boundary-crossing particle (Eq. 3.28 respectively).

[1] A basic mathematical criterion that determines whether a mixed finite element discretization is stable and convergent.

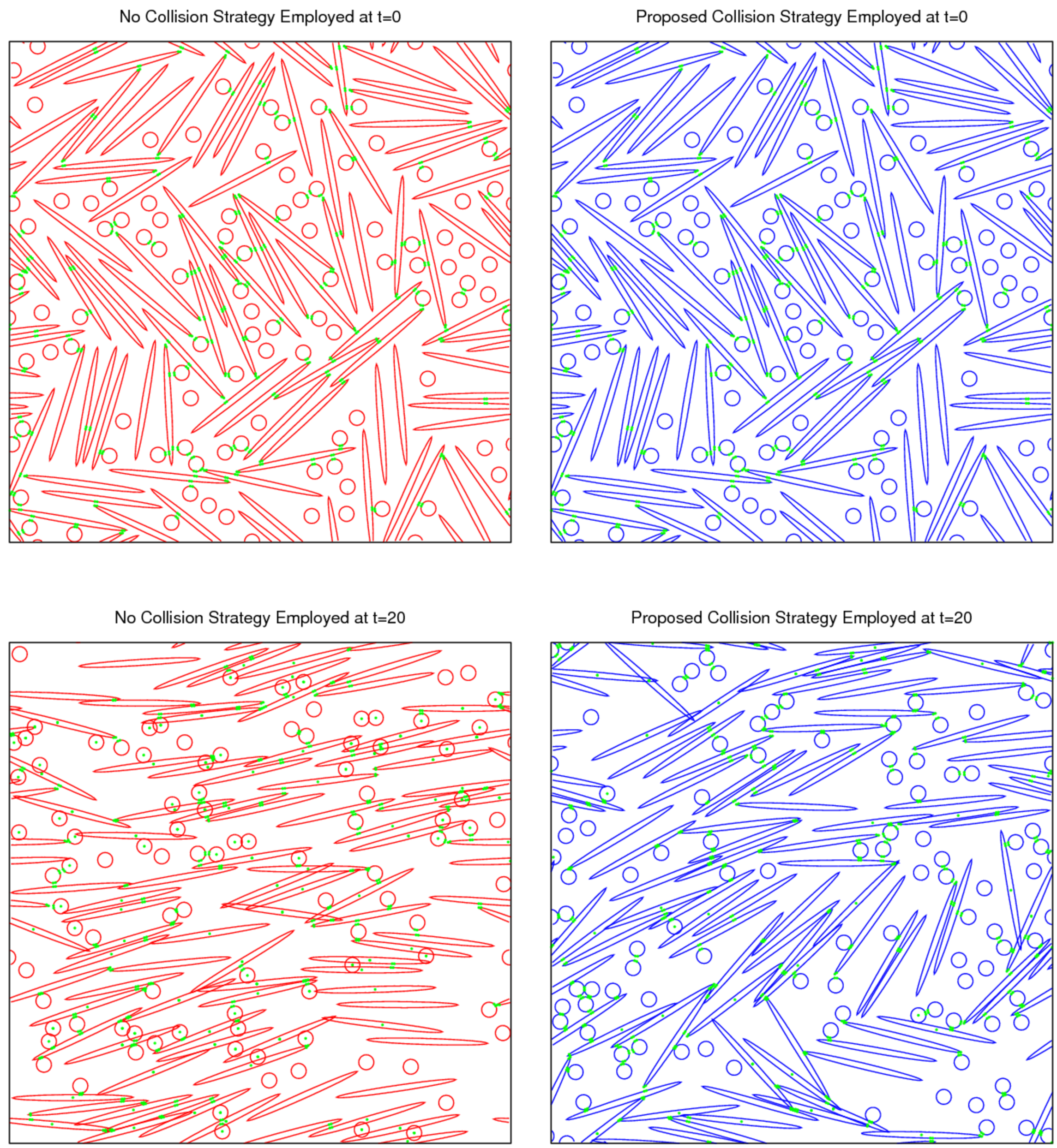

Figure 3.7: The proposed collision strategy significantly reduces inter-fiber intersection. The green dots along fiber surfaces denote near-collision points, and the ones in the centers of the fibers denote on-going intersections. (aspect ratio: 20, $vol\%_{particle} = 7\%$ and $vol\%_{fiber} = 20\%$)

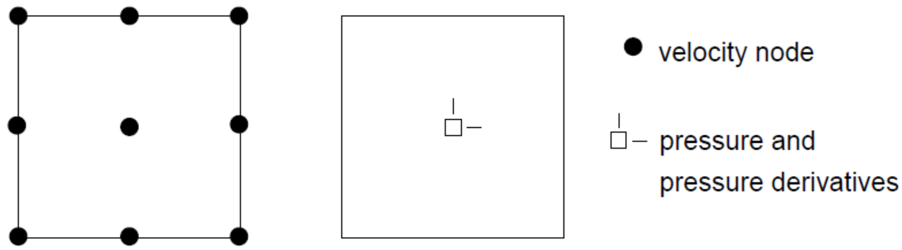

Figure 3.8: A $Q_2 - P_1^d$ element in a regular rectangular discretization with the bi-quadratic interpolation of the velcity and the linear discontinuous interpolation for the pressure. (Reproduced with permission: Hwang et al., 2004. [38])

3.3.3 Time integration

We employ explicit time integration schemes — the explicit Euler method at the first time step and the second-order Adams-Bashforth method from the second time step. A modified second-order Adams-Bashforth scheme for the particle P_i which comes from the upper or lower boundary, in the x-direction

$$X_i^{n+1} \approx X_i'^n + \Delta t\,(\frac{3}{2}U_i^n - \frac{1}{2}U_i'^{n-1}) \tag{3.33}$$

where X_i^{n+1}, $X_i'^n$, U_i^n, $U_i'^{n-1}$ are the present particle position, the next step particle position, the present velocity and the modified previous velocity respectively.

3.4 Collocation Points

It can be tricky when it comes to deciding the number of collocation points along the surface of a fiber. Unlike the example problem shown in Hwang et al.'s work [38], with circular particles not colliding, elliptical fibers don't have a constant curvature, so the linear velocity of one point varies largely from another, rendering it much more inclined to collisions. The number of collocation points along a fiber/particle is chosen such that the average number of collocation point in each element is ~1.13 throughout this study (Table 3.2).

Table 3.2: Number of collocation points used for fibers

major axis	minor axis	aspect ratio	number of collocation points
0.030	0.030	1	20
0.012	0.216	18	96
0.012	0.240	20	108
0.012	0.264	22	120

Finite Element based simulation was performed using the above approach developed and provided by Hwang et al. [38, 39, 40], and the simulation results of various studies are discussed in the next chapter.

Chapter 4

SIMULATION RESULTS

4.1 Simulation Plans

In order to reveal the disparity between fiber orientations with and without circular particles in the system undergoing a simple shear flow, the simulation experiments are conducted as follows:

Step 1. Run simulations with only fibers $\text{vol\%}_{\text{fiber}}$ in the suspension. Observe the fiber orientations a_{ij} evolve over time, and calculate C_I^{fiber}.

Step 2. Run simulations with both fibers $\text{vol\%}_{\text{fiber}}$ and particles $\text{vol\%}_{\text{particle}}$ in the suspension. Observe the fiber orientations ${a_{ij}}^{\text{fiber w/ particle}}$ evolve over time, and calculate the according $C_I^{\text{fiber w/ particle}}$.

Step 3. Repeat **step 1** and **step 2** for other combinations of C_I^{fiber} and $C_I^{\text{fiber w/ particle}}$. Plot the results. Configurations for fiber-only suspensions are shown in Table 4.1, and fiber-particle suspensions are shown in Table 4.2.

Step 4. Compare the simulation C_I^{fiber} with those from other existing models.

Step 5. Compare the results C_I^{fiber} and $C_I^{\text{fiber w/ particle}}$. Study the difference induced by the presence of the circular particles in the system.

The simulations in this work are conducted on the High Performance Cluster (HPC) “Mills” on the University of Delaware campus. The realizations of the simulations are derived from a series of FORTRAN routines kindly provided by Hwang et al. [38, 39, 40].

Table 4.1: Simulation configurations for fiber-only suspensions

major axis	minor axis	aspect ratio	$\text{vol\%}_{\text{fiber}}$	Δt	# of time steps
0.216	0.012	18			
0.240	0.012	20	7%, 15%, 20%	0.05	600
0.264	0.012	22			

Table 4.2: Simulation configurations for fiber-particle suspensions

major axis	minor axis	aspect ratio	$\text{vol\%}_{\text{fiber}}$	$\text{vol\%}_{\text{particle}}$	Δt	# of time steps
0.216	0.012	18		6%, 8%,		
0.240	0.012	20	15%	10%, 12%,	0.05	600
0.264	0.012	22		14%		

Following additions, functions and revisions to accomplish the research objectives were introduced by me to address the issue of collisions.

- recognizing boundary-crossing ellipses and constructing "virtual ring"s of them for inter-ellipse distance calculation
- determining the minimum distance between two ellipses in any simulation zone and at any angle, and exerting a force-pair to the collocation points along the surface of the ellipse-pair that are too close
- detecting intersection of two ellipses and applying an additional velocity (and angular velocity) to the center of the represented fibers/particles
- for the initial step $t = 0$, identifying ellipses with equal axes (i.e., circular particles), initializing them with $\theta = 0$, and excluding them from the calculation of orientation tensor $\boldsymbol{A}$
- for the initial step $t = 0$, identifying ellipses with non-equal axes (i.e., elliptical fibers), initializing them with randomized θ making $a_{11}|_{t=0} = 0.5$
- reading the pre-set orientation and position distribution of fibers from files
- allowing for larger domain size and matrix computations
- resuming from a previous simulation for more efficient use of the HPC resources
- outputting specified information for post-processing

4.2 Simulation Results

The direct bi-period simulation provided the velocity field (Eq. 3.3.2) of the matrix, and the complete information of the rigid-body motions. The orientation tensor can then be directly calculated from Eq. 2.13 to 2.15. Then, C_I can be calculated from Eq. 2.39.

For each combination of fiber and circular particle concentrations, $\sim$30 simulations are conducted with randomized initial location and orientation, with $a_{11}\big|_{t=0} = 0.5$. At least 119 fibers are present in each computation domain to ensure a smooth fiber orientation transition. The variance in the concentration is achieved by varying the sizes of the computation domain Ω.

Preliminary results show that, from the initial random state, C_I decreases drastically from larger than $O(10^0)$ to $O(10^{-3})$ as the fibers align (Figure 4.1). Because the equation used to calculate C_I (Eq. 2.39) has the term $(1-2a_{11})$ in the denominator, C_I becomes negative when $a_{11} < 0.5$, which is not shown in the log-scale. This decrease in C_I is supported by the numerical results reported by Ranganathan and Advani [31], who associate the inter-fiber rotary diffusion with inter-fiber spacing, and show that the orientation dependent interaction coefficient C_I describes a delayed alignment than the constant. All C_I reported in this work is the steady-state C_I, which is calculated when the variances of C_I and a_{11} become stable.

4.2.1 Circular particle only suspension system

Figure 4.2 plots the relative viscosity $\langle\eta\rangle/\eta$ as a function of the volume fraction of circular particle vol%$_{\text{particle}}$. In this work, the radii of all circular particles are 0.03.

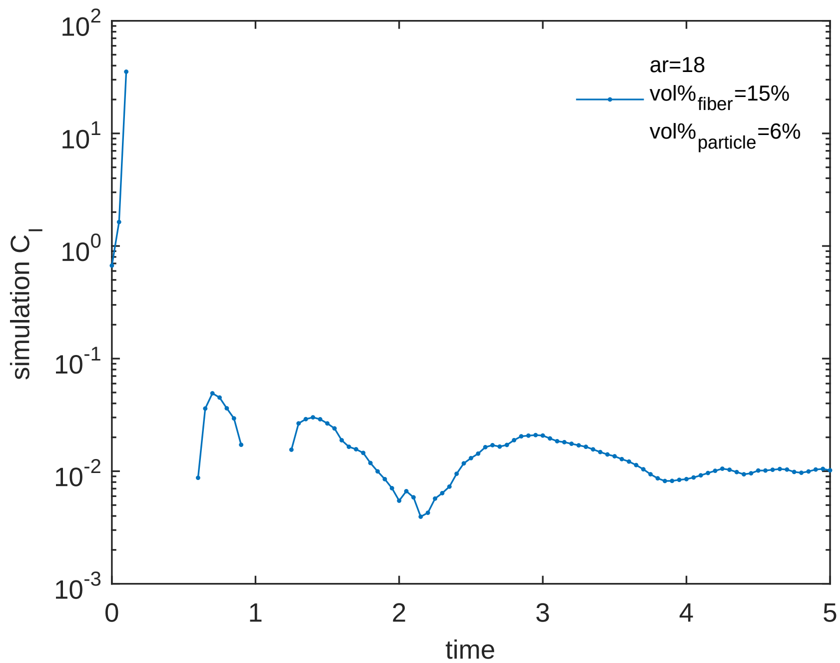

Figure 4.1: Non-averaged simulation result C_I is plotted as a function of time.

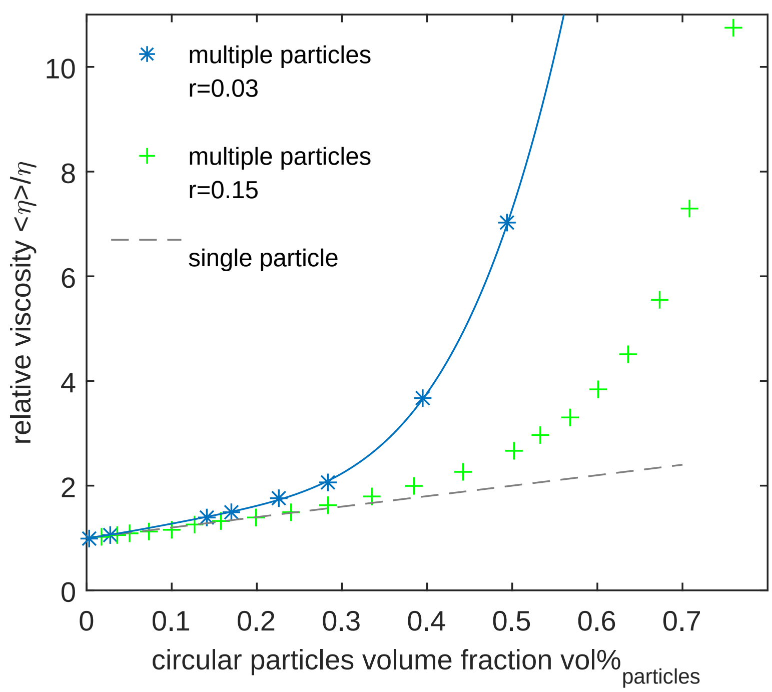

Figure 4.2: The relative viscosity for circular particles suspensions with increasing vol%$_{\text{particle}}$

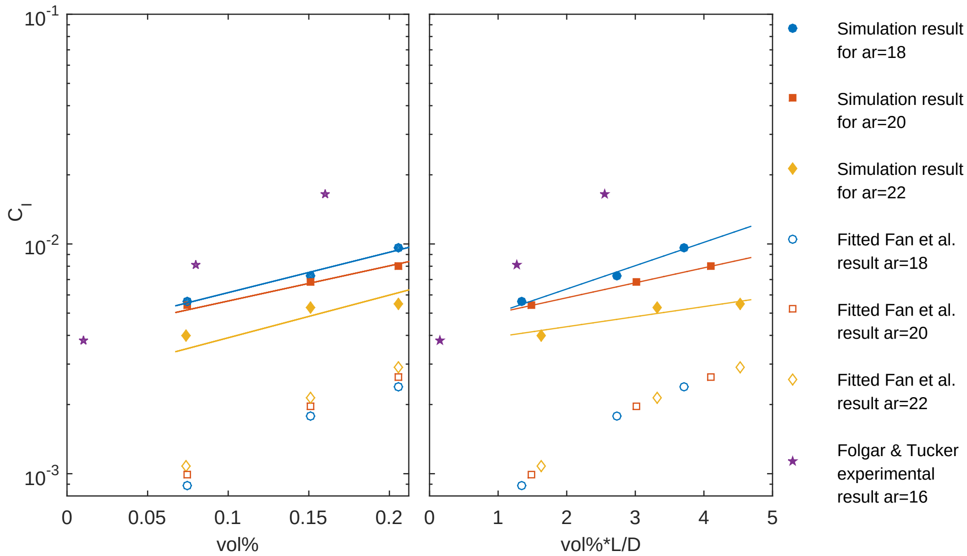

Figure 4.3: The computed interaction coefficient C_I of neat fiber suspension system, with aspect ratio 18, 20 and 22, plotted against two concentration parameters - volume fraction vol%$_{\text{fiber}}$ (*left*), and vol%$_{\text{fiber}}$ L/D (*right*). For comparison purposes, the experimental results of Folgar and Tucker for ar=16, and the fitted value from Fan et al.'s simulation model are also plotted.

4.2.2 Neat fiber suspension system

Figure 4.3 plots the steady-state interaction coefficient C_I of neat fiber suspension system with aspect ratio 18, 20 and 22, against two concentration parameters — vol%$_{\text{fiber}}$ on the left, and vol%$_{\text{fiber}}$ L/D on the right. All C_Is obtained from simulations span roughly within the $O(10^{-3}) \sim O(10^{-2})$ range. In both plots, the steady-state C_I increases exponentially as the concentration of fibers does. And it decreases as the fibers increase in aspect ratio.

All simulation data are least-squares-fitted with exponential models per two concentration parameters respectively, hence the discrepancy in slopes.

Folgar and Tucker experimental results with aspect ratio 16 are also plotted in the figure with filled stars.

The aspect ratios and volume fractions used in the simulations are used in Fan et al.'s fitted model, and plotted with unfilled markers in Figure 4.3. Their actual experimental results are not illustrated here. It's worth mentioning that, although their fitted model suggest that a larger aspect ratio with constant fiber volume fraction incurs a greater diffusivity (Eq. 2.5), their pre-fitted simulation dataset suggests otherwise.

4.2.3 Fiber-particle suspension system

In this section. we use $C_I^{\text{fiber w/ particle}}$ to represent the steady-state interaction coefficient C_I of the fibers suspended in a particle-loaded system. Here we need to clarify that, the calculation of C_I, or more directly the $\boldsymbol{A}$ components, doesn't involve the orientation of the circular particles, as it does not carry any physical meanings. The words "w/ particle" are to stress the differences in the suspension constituents.

In Figure 4.4, we exhibit $C_I^{\text{fiber w/ particle}}$ for fiber-particles suspensions of 3 aspect ratios. Maintaining a vol%$_{\text{fiber}} \approx 15\%$ for all data points, we plot the according coefficients with ascending vol%$_{\text{particle}}$ from 6% to 14%. Again, all simulation data are least-squares-fitted with exponential models, shown as solid lines in the figure. Because the aspect ratio for the circular particles is 1, no plot against vol%$_{\text{fiber}}$ L/D is presented.

As for the alignment of the fibers, an example of the averaged a_{11} is shown in Figure 4.5. It's evident to see that, as the circular particles amass, the fibers are to undergo a more vigorous rotary diffusion.

Figure 4.6 compares the constant C_I models of linear and quadratic approximations with the simulation result $C_I^{\text{fiber w/ particle}}$. As discussed before, the $C_I^{\text{fiber w/ particle}}$ proves to be exceedingly large when the fibers randomly orientate. Using the steady state

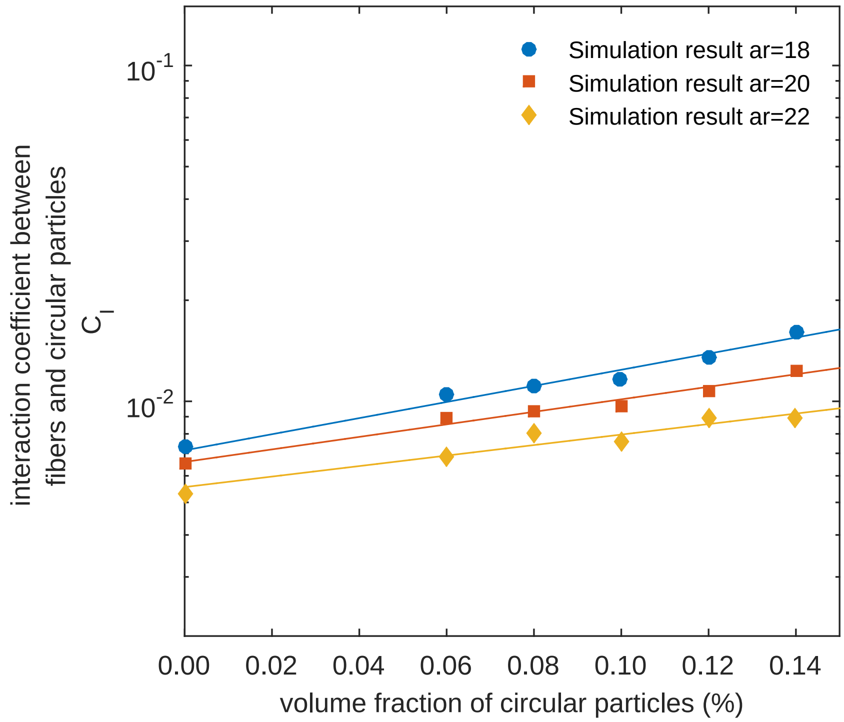

Figure 4.4: The computed interaction coefficient C_I of hybrid fiber-particle suspension system, with aspect ratio 18, 20 and 22, plotted against the volume fraction vol%$_{\text{particle}}$. For all data points in this plot, vol%$_{\text{fiber}} \approx 15\%$

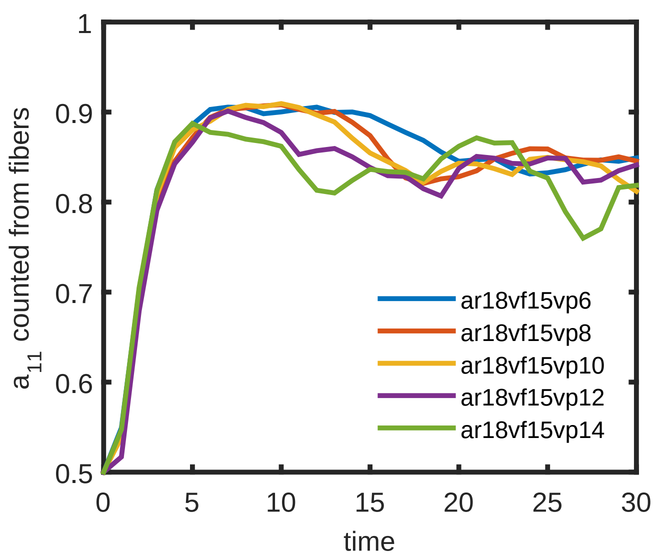

Figure 4.5: Simulation results of a_{11} as a function of time t for suspension system with identical vol%$_{\text{fiber}}$ but growing vol%$_{\text{particle}}$

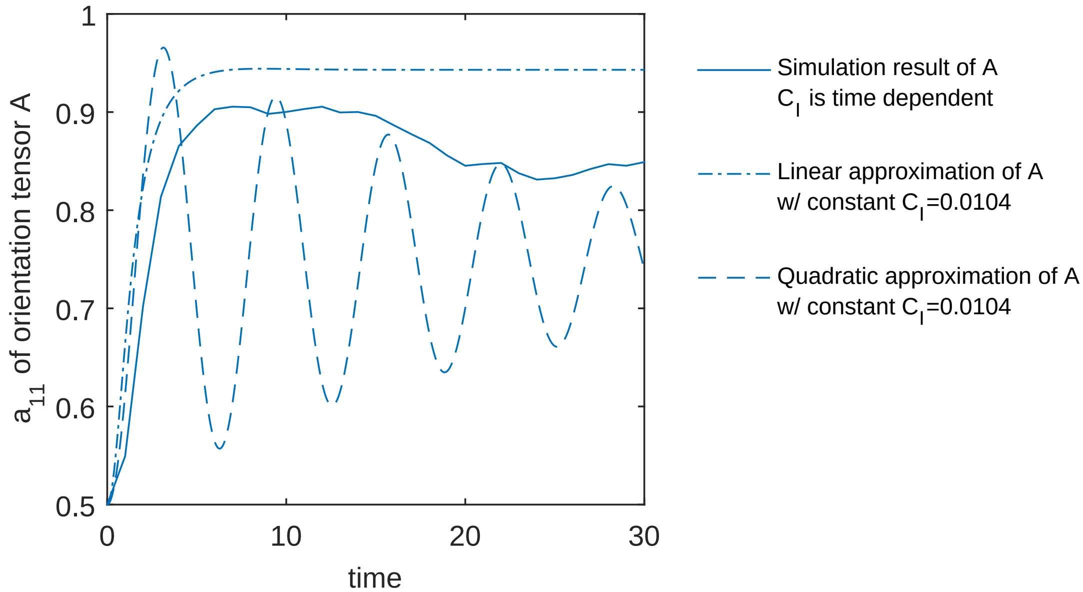

Figure 4.6: Simulation result a_{11} is plotted as a function of time. Visualized data is collected from simulation of ar=18, vol%$_{\text{fiber}}$ =15% , vol%$_{\text{particle}}$ =6%. The dotted lines are the numerical result derived with constant C_I using quadratic and hybrid approximations.

$C_I^{\text{fiber w/ particle}}$ from the simulation, neither of these constant C_I models accurately predict the dynamics of fiber orientation.

4.3 Discussion

In this work, no approximation is necessary to calculate the transient ${}^4\boldsymbol{A}$ tensor components, as all of them can be directly obtained from the instantaneous fiber orientation (Eq. 2.15).

Figure 4.4 clearly shows that, the presence of the circular particles alters the track of the fibers aligning and introduces more random behavior into the system.

It is safe to conclude that, fibers suspended in a non-dilute particle suspension will experience a stronger resistance from aligning in the flow direction. This means that, simply taking the effective viscosity of a particle suspension does not necessarily tell the whole story of the fiber orientation, which is critical when it comes to the mechanical properties of the manufactured articles.

Chapter 5

CONCLUSIONS AND FUTURE WORK

5.1 Summary and Conclusions

The orientation of the force-free torque-free fibers suspended in a circular-particle-loaded suspension undergoing a simple shear flow in a Newtonian matrix is studied. This problem is modeled by a direct bi-periodic simulation domain packed with elliptical and circular disks inside. A dedicated collision strategy for elliptical fibers is developed and employed for non-dilute suspension using this simulation method. With given random initial locations and orientations of the fibers and the particles, the finite element method solves a series of balance equations and boundary constraints for the complete flow field and the rigid-body areas. It then moves on to the next step through a similar procedure, until a desirable length of simulation is completed. For each time step, the orientation of all the fibers are analyzed and used to calculate the instantaneous interaction coefficient C_I.

The interaction coefficient C_I is shown to be time dependent, which can be explained by theories of fiber interactions being dependent on inter-fiber spacing. A comparison between constant C_I model and the simulation result show that the constant C_I doesn't predict the fiber orientation to one's satisfaction.

C_I^{fiber} for varying aspect ratios and vol%$_{\text{fiber}}$ are inspected and compared with other established fiber suspension models. A positive correlation is found between the steady state C_I^{fiber} and the vol%$_{\text{fiber}}$, and a negative correlation is found between C_I^{fiber} and the aspect ratio of the fibers.

The existence of circular particles suspended in the resin impact the fiber orientation process due to the collision experienced. The fiber orientation is slow to align in the direction of the shear due to the presence of particles. The degree of alignment decreases as the concentration of particles increases. This is then demonstrated and verified by comparing the $C_I^{\text{fiber w/ particle}}$s and the orientation tensor evolution between increasing particle content systems.

5.2 Future Work

This work restricts itself to a 2-dimensional domain, which largely restricted the motions of fibers and the circular particles. Fan et al.'s work confirms that, for a semi-concentrated regime in a 3-dimensional domain, the fiber trajectory constantly rotates out of the xy-plane [33], which allows the fiber more spacial flexibility to not tangle up with other ones. If this is implemented, the ad-hoc collision strategy (especially the post-collision part) might have a less significant affect on the stress calculation.

Most of the C_I reported are plotted as functions of both volume fraction of the fibers and vol%$_{\text{fiber}}$ L/D, it seems that, in vol%$_{\text{fiber}}$ L/D graphs, C_I is generally larger with smaller aspect ratio. However, most models fitted with experimental results do not recognize this phenomenon. If enough data is collected, one could arguably fit an exponential model for each aspect ratio, then fit the parameters of those models to be functions of the aspect ratios of the fibers, to obtain a final model.

At this moment, the $C_I^{\text{fiber w/ particle}}$ data is not sufficient to build a model for the particle-loaded fiber suspensions. But it is sensible to run simulations for a large set of volume fractions of both fibers and circular particles, and build a model in the form

$$C_I^{\text{fiber w/ particle}} = C_I^{\text{particle contribution}} + C_I^{\text{fiber contribution}} \tag{5.1}$$

BIBLIOGRAPHY

[1] M. F. Ashby, S. F. Bush, N. Swindells, R. Bullough, G. Ellison, Y. Lindblom, R. W. Cahn, and J. F. Barnes, “Technology of the 1990s: Advanced Materials and Predictive Design [and Discussion],” *Philosophical Transactions of the Royal Society A: Mathematical, Physical and Engineering Sciences*, vol. 322, pp. 393–407, jul 1987.

[2] C. L. Tucker III and S. G. Advani, “Processing of short-fiber systems,” in *Flow and Rheology in Polymer Composites Manufacturing*, 1994.

[3] PlastiComp, Inc. `www.plasticomp.com`, 2015.

[4] A. Einstein, “Eine neue bestimmung der moleküldimensionen,” *Ann. Physik*, no. 19, pp. 289–306, 1906.

[5] G. B. Jeffery, “The motion of ellipsoidal particles immersed in a viscous fluid,” *Proceedings of the Royal Society A: Mathematical, Physical and Engineering Sciences*, vol. 102, pp. 161–179, nov 1922.

[6] F. P. Bretherton, “The motion of rigid particles in a shear flow at low Reynolds number,” *Journal of Fluid Mechanics*, vol. 14, no. 02, pp. 284–304, 1962.

[7] R. G. Cox, “The motion of long slender bodies in a viscous fluid. Part 2. Shear flow,” *Journal of Fluid Mechanics*, vol. 45, p. 625, mar 2006.

[8] J. B. Harris and J. F. T. Pittman, “Equivalent ellipsoidal axis ratios of slender rod-like particles,” *Journal of Colloid and Interface Science*, vol. 50, no. 2, pp. 280–282, 1975.

[9] G. K. Batchelor, “The stress system in a suspension of force-free particles,” *Journal of fluid mechanics*, vol. 41, no. 03, pp. 545–570, 1970.

[10] E. J. Hinch and L. G. Leal, “The effect of Brownian motion on the rheological properties of a suspension of non-spherical particles,” *Journal of Fluid Mechanics*, vol. 62, pp. 683–712, 1972.

[11] S. M. Dinh and R. C. Armstrong, “A rheological equation of state for semiconcentrated fiber suspensions,” *Journal of Rheology (1978-present)*, vol. 28, p. 207, jun 1984.

[12] E. S. G. Shaqfeh and G. H. Fredrickson, “The hydrodynamic stress in a suspension of rods,” *Physics of Fluids A: Fluid Dynamics*, vol. 2, pp. 7–24, jan 1990.

[13] D. L. Koch and E. S. G. Shaqfeh, “The average rotation rate of a fiber in the linear flow of a semidilute suspension,” *Physics of Fluids A: Fluid Dynamics (1989-1993)*, vol. 2, no. 12, pp. 2093–2102, 1990.

[14] E. S. G. Shaqfeh and D. L. Koch, “Orientational dispersion of fibers in extensional flows,” *Physics of Fluids A: Fluid Dynamics*, vol. 2, no. 7, p. 1077, 1990.

[15] M. Doi and S. F. Edwards, “Dynamics of rod-like macromolecules in concentrated solution Part 1,” *Journal of the Chemical Society, Faraday Transactions 2: Molecular and Chemical Physics*, vol. 74, no. 6, pp. 560–570, 1978.

[16] M. Doi and S. F. Edwards, “Dynamics of rod-like macromolecules in concentrated solution. Part 2,” *Journal of the Chemical Society, Faraday Transactions 2: Molecular and Chemical Physics*, vol. 74, no. 6, pp. 918–932, 1978.

[17] F. Folgar and C. L. Tucker III, “Orientation behavior of fibers in concentrated suspensions,” *Journal of Reinforced Plastics and Composites*, vol. 3, no. 2, p. 98, 1984.

[18] R. S. Bay, *Fiber orientation in injection molded composites: A comparison of theory and experiment*. PhD thesis, 1991.

[19] A. W. K. Ma, F. Chinesta, and M. R. Mackley, “The rheology and modeling of chemically treated carbon nanotubes suspensions,” *Journal of Rheology*, vol. 53, no. 3, p. 547, 2009.

[20] S. G. Advani and C. L. Tucker III, “The use of tensors to describe and predict fiber orientation in short fiber composites,” *Journal of Rheology*, vol. 31, no. 8, p. 751, 1987.

[21] S. Ranganathan and S. G. Advani, “Characterization of orientation clustering in short-fiber composites,” *Journal of Polymer Science Part B: Polymer Physics*, vol. 28, pp. 2651–2672, dec 1990.

[22] X. Cheng, X. Xu, S. A. Rice, A. R. Dinner, and I. Cohen, “Assembly of vorticity-aligned hard-sphere colloidal strings in a simple shear flow.,” *Proceedings of the National Academy of Sciences of the United States of America*, vol. 109, pp. 63–67, jan 2012.

[23] S. G. Advani and C. L. Tucker III, “Closure approximations for three-dimensional structure tensors,” *Journal of Rheology*, vol. 34, pp. 367–386, apr 1990.

[24] V. Verleye and F. Dupret, “Prediction of fiberorientation in complex injection molded parts,” in *Developments in Non-Newtonian Flows* (D. A. Siginer, W. E. VanArsdale, M. C. Altan, and A. N. Alexandrou, eds.), vol. AMD-Vol. 1, pp. 139–163, ASME, 1993.

[25] F. Dupret and V. Verleye, “Modelling the flow of fiber suspensions in narrow gaps,” in *Advances in the Flow and Rheology of Non-Newtonian Fluids* (D. Siginer, D. D. Kee, and R. P. Chhabra, eds.), vol. 8, pp. 1347–1398, Elsevier, 1999.

[26] J. S. Cintra Jr. and C. L. Tucker III, “Orthotropic closure approximations for flow-induced fiber orientation,” *Journal of Rheology*, vol. 39, p. 1095, nov 1995.

[27] D. H. Chung and T. H. Kwon, “Invariant-based optimal fitting closure approximation for the numerical prediction of flow-induced fiber orientation,” *Journal of Rheology*, vol. 46, p. 169, jan 2002.

[28] K.-H. Han and Y.-T. Im, “Modified hybrid closure approximation for prediction of flow-induced fiber orientation,” *Journal of Rheology*, vol. 43, p. 569, may 1999.

[29] B. O. Agboola, “Investigation of dense suspension rotary diffusion models for fiber orientation predictions during injection molding of short-fiber reinforced polymeric composites.,” 2011.

[30] S. Montgomery-Smith, D. Jack, and D. E. Smith, “The Fast Exact Closure for Jeffery’s equation with diffusion,” *Journal of Non-Newtonian Fluid Mechanics*, vol. 166, pp. 343–353, apr 2011.

[31] S. Ranganathan and S. G. Advani, “Fiber-fiber interactions in homogeneous flows of nondilute suspensions,” *Journal of Rheology*, vol. 35, no. November, p. 1499, 1991.

[32] Y. Yamane, Y. Kaneda, and M. Doi, “Numerical simulation of semi-dilute suspensions of rodlike particles in shear flow,” *Journal of Non-Newtonian Fluid Mechanics*, vol. 54, pp. 405–421, aug 1994.

[33] X. Fan, N. Phan-Thien, and R. Zheng, “A direct simulation of fibre suspensions,” *Journal of Non-Newtonian Fluid Mechanics*, vol. 74, no. 1-3, pp. 113–135, 1998.

[34] N. Phan-Thien, X. Fan, R. Tanner, and R. Zheng, “Folgar–Tucker constant for a fibre suspension in a Newtonian fluid,” *Journal of Non-Newtonian Fluid Mechanics*, vol. 103, no. 2-3, pp. 251–260, 2002.

[35] D. L. Koch, “A model for orientational diffusion in fiber suspensions,” *Physics of Fluids*, vol. 2086, no. 1995, pp. 100–102, 1995.

[36] N. Phan-Thien, X. Fan, and R. Zheng, “A numerical simulation of suspension flow using a constitutive model based on anisotropic interparticle interactions,” *Rheologica acta*, vol. 39, no. 2, pp. 122–130, 2000.

[37] J. H. Phelps and C. L. Tucker III, "An anisotropic rotary diffusion model for fiber orientation in short-and long-fiber thermoplastics," *Journal of Non-Newtonian Fluid Mechanics*, vol. 156, no. 3, pp. 165–176, 2009.

[38] W. R. Hwang, M. A. Hulsen, and H. E. Meijer, "Direct simulation of particle suspensions in sliding bi-periodic frames," *Journal of Computational Physics*, vol. 194, pp. 742–772, mar 2004.

[39] W. R. Hwang, M. A. Hulsen, and H. E. Meijer, "Direct simulations of particle suspensions in a viscoelastic fluid in sliding bi-periodic frames," *Journal of Non-Newtonian Fluid Mechanics*, vol. 121, no. 1, pp. 15–33, 2004.

[40] H. Chung, S. Kang, and W. R. Hwang, "Numerical simulations of elliptic particle suspensions in sliding bi-periodic frames," *Korea-Australia Rheology Journal*, vol. 17, no. 4, pp. 171–180, 2005.

[41] C. Bernardi, Y. Maday, and A. T. Patera, "A new nonconforming approach to domain decomposition: The mortar element method," in *Nonlinear partial differential equations and their applications. Coll{è}ge de France Seminar, volume XI. Lectures presented at the weekly seminar on applied mathematics*, pp. 13–51, 1994.

[42] F. B. Belgacem and Y. Maday, "The mortar element method for three dimensional finite elements," *ESAIM: Mathematical Modelling and Numerical Analysis - Modélisation Mathématique et Analyse Numérique*, vol. 31, no. 2, pp. 289–302, 1997.

[43] F. P. T. Baaijens, "A fictitious domain/mortar element method for fluid-structure interaction," *International Journal for Numerical Methods in Fluids*, vol. 35, pp. 743–761, apr 2001.

[44] R. Glowinski, T. W. Pan, T. I. Hesla, and D. D. Joseph, "A distributed Lagrange multiplier/fictitious domain method for particulate flows," *International Journal of Multiphase Flow*, vol. 25, no. 5, pp. 755–794, 1999.

[45] P. Laure, A. Megally, and T. Coupez, "Collision strategy for the direct simulation of moving fibers in viscous fluid," *Int. Conf. Comput. Problems in Sci & Engrg.*, pp. 1–13, 2005.

[46] S. Rezak, *Analysis of flexible fiber suspensions using the Lattice Boltzmann method*. PhD thesis, Georgia Institute of Technology, 2008.

[47] I.-S. Kim, "An Algorithm for Finding the Distance Between Two Ellipses," *Communications of the Korean Mathematical Society*, vol. 21, no. 3, pp. 559–567, 2006.

Appendix A

DIRECT CALCULATION OF C_I

The 4 components of C_I being calculated from the simulations can be derived from (2.32), written here again:

$$\frac{\mathrm{D}a_{ij}}{\mathrm{D}t} + \frac{1}{2}\big(\omega_{ik}a_{kj} - a_{ik}\omega_{kj}\big) = \frac{1}{2}\lambda\big(\dot{\gamma}_{ik}a_{kj} + a_{ik}\dot{\gamma}_{kj} - 2\dot{\gamma}_{kl}a_{ijkl}\big) + 2C_I\dot{\gamma}\big(\delta_{ij} - \alpha a_{ij}\big)$$

with simplified flow parameters ω_{ij} and $\dot{\gamma}_{ij}$ for the simple shear flow being

$$\dot{\gamma}_{ij} = \begin{bmatrix} \dfrac{\partial v_1}{\partial x_1} + \dfrac{\partial v_1}{\partial x_1} & \dfrac{\partial v_2}{\partial x_1} + \dfrac{\partial v_1}{\partial x_2} \\ \dfrac{\partial v_1}{\partial x_2} + \dfrac{\partial v_2}{\partial x_1} & \dfrac{\partial v_2}{\partial x_2} + \dfrac{\partial v_2}{\partial x_2} \end{bmatrix} = \begin{bmatrix} 0 & \dot{\gamma} \\ \dot{\gamma} & 0 \end{bmatrix} \tag{A.1}$$

$$\omega_{ij} = \begin{bmatrix} \dfrac{\partial v_1}{\partial x_1} - \dfrac{\partial v_1}{\partial x_1} & \dfrac{\partial v_2}{\partial x_1} - \dfrac{\partial v_1}{\partial x_2} \\ \dfrac{\partial v_1}{\partial x_2} - \dfrac{\partial v_2}{\partial x_1} & \dfrac{\partial v_2}{\partial x_2} - \dfrac{\partial v_2}{\partial x_2} \end{bmatrix} = \begin{bmatrix} 0 & -\dot{\gamma} \\ \dot{\gamma} & 0 \end{bmatrix} \tag{A.2}$$

Now, examine the terms of (2.32).

When $i = 1,$ and $j = 1,$

$$\begin{aligned}
\text{L.H.S} &= \frac{\mathrm{D}a_{11}}{\mathrm{D}t} + \frac{1}{2}(\omega_{1k}a_{k1} - a_{1k}\omega_{k1}) \\
&= \frac{\mathrm{D}a_{11}}{\mathrm{D}t} + \frac{1}{2}(\omega_{11}a_{11} + \omega_{12}a_{21} - a_{11}\omega_{11} - a_{12}\omega_{21}) \\
&= \frac{\mathrm{D}a_{11}}{\mathrm{D}t} + \frac{1}{2}(0 - \dot{\gamma}a_{21} - 0 - a_{12}\dot{\gamma}) \\
&= \frac{\mathrm{D}a_{11}}{\mathrm{D}t} - \dot{\gamma}a_{12} \\
\text{R.H.S} &= \frac{1}{2}\lambda(\dot{\gamma}_{1k}a_{k1} + a_{1k}\dot{\gamma}_{k1} - 2\dot{\gamma}_{kl}a_{11kl}) + 2C_I\dot{\gamma}(\delta_{11} - 2a_{11}) \\
&= \frac{1}{2}\lambda(\dot{\gamma}_{11}a_{11} + \dot{\gamma}_{12}a_{21} + a_{11}\dot{\gamma}_{11} + a_{12}\dot{\gamma}_{21} \\
&\quad -2\dot{\gamma}_{11}a_{1111} - 2\dot{\gamma}_{12}a_{1112} - 2\dot{\gamma}_{21}a_{1121} - 2\dot{\gamma}_{22}a_{1122}) \\
&\quad +2C_I\dot{\gamma}(1 - 2a_{11}) \\
&= \frac{1}{2}\lambda(0 + \dot{\gamma}_{12}a_{21} + 0 + a_{12}\dot{\gamma}_{21} \\
&\quad -0 - 2\dot{\gamma}_{12}a_{1112} - 2\dot{\gamma}_{21}a_{1121} - 0) \\
&\quad +2C_I\dot{\gamma}(1 - 2a_{11}) \\
&= \lambda(\dot{\gamma}a_{12} - 2\dot{\gamma}a_{1112}) + 2C_I\dot{\gamma}(1 - 2a_{11})
\end{aligned}$$

Then,

$$C_{I_{11}} = \frac{\dfrac{\partial a_{11}}{\partial t} - (1+\lambda)\dot{\gamma}a_{12} + 2\lambda\dot{\gamma}a_{1112}}{2\dot{\gamma}(1 - 2a_{11})} \tag{A.3}$$

Similarly,

$$
\begin{aligned}
C_{I_{11}} &= \frac{\dfrac{\partial a_{11}}{\partial t} - (1+\lambda)\dot{\gamma} a_{12} + 2\lambda\dot{\gamma} a_{1112}}{2\dot{\gamma}(1-2a_{11})} \\
C_{I_{22}} &= \frac{\dfrac{\partial a_{11}}{\partial t} - (1+\lambda)\dot{\gamma} a_{12} + 2\lambda\dot{\gamma} a_{1112}}{2\dot{\gamma}(1-2a_{11})} \\
C_{I_{12}} &= \frac{-\dfrac{\partial a_{12}}{\partial t} - \dfrac{\dot{\gamma}}{2}(2a_{11} - \lambda - 1) - 2\lambda\dot{\gamma} a_{1122}}{4\dot{\gamma} a_{12}} \\
C_{I_{21}} &= \frac{-\dfrac{\partial a_{12}}{\partial t} - \dfrac{\dot{\gamma}}{2}(2a_{11} - \lambda - 1) - 2\lambda\dot{\gamma} a_{1122}}{4\dot{\gamma} a_{12}}
\end{aligned}
\tag{A.4}
$$

Appendix B

REMARKS ON THE CHOICE OF USING $C_{I_{11}}$ AS C_I

B.1 Preliminary Result

For each step, $C_{I_{11}}$ and $C_{I_{12}}$ can be directly calculated from Eq. 2.39, rewritten here:

$$C_{I_{11}} = \frac{\dfrac{\partial a_{11}}{\partial t} - (1+\lambda)\dot{\gamma}a_{12} + 2\lambda\dot{\gamma}a_{1112}}{2\dot{\gamma}(1-2a_{11})}$$

$$C_{I_{12}} = \frac{-\dfrac{\partial a_{12}}{\partial t} - \dfrac{\dot{\gamma}}{2}(2a_{11} - \lambda - 1) - 2\lambda\dot{\gamma}a_{1122}}{4\dot{\gamma}a_{12}}$$

As shown in Figure B.1, the $C_{I_{11}}$ and $C_{I_{12}}$ both start off with great deviations when the fibers are randomly orientated, but then they develop distinct patterns as the fiber orientation evolves — the deviation of $C_{I_{11}}$ reduces and remains relatively steady when compared with that of $C_{I_{12}}$.

B.2 Explanations for the Distinct Behaviors of $C_{I_{11}}$ and $C_{I_{12}}$

The discrepancy of these two quantities $C_{I_{11}}$ and $C_{I_{12}}$ can be explained by the way they are calculated.

As shown in Eq. 2.39, the values of $C_{I_{11}}$ at $a_{11} = 0.5$ and $C_{I_{12}}$ at $a_{12} = 0$ become infinity. This directly affects the values of these C_I components and poses a **stability** issue when using $C_{I_{12}}$ as C_I.

Moreover, the sensitivity of C_I components to their variables (i.e., $\dfrac{\partial C_{I_{11}}}{\partial f_i}$, $\dfrac{\partial C_{I_{12}}}{\partial g_i}$, …, where f_i and g_i are the independent variables of $C_{I_{11}}$ and $C_{I_{12}}$ respectively) are,

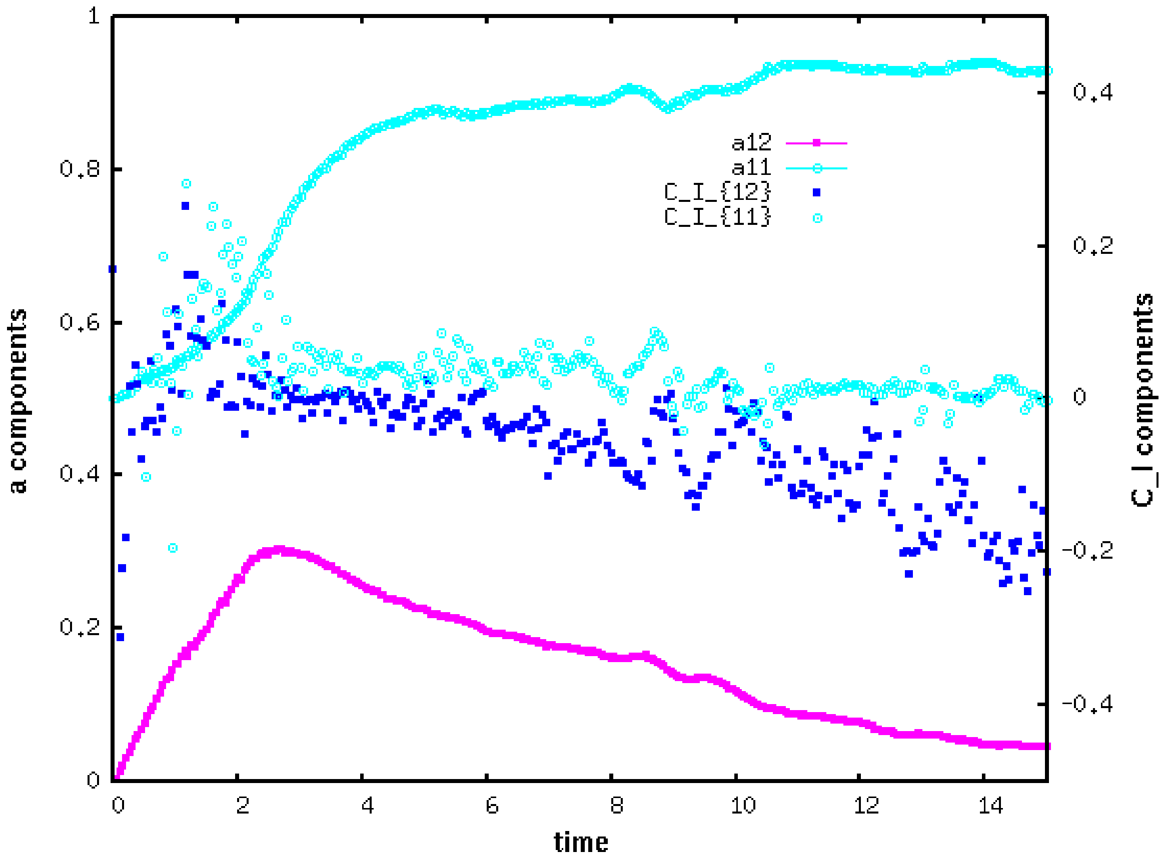

Figure B.1: A typical result of the evolution of orientation tensor components (a_{11} and a_{12}, y axis on the left) and that of C_I components ($C_{I_{11}}$ and $C_{I_{12}}$, y axis on the right). The magenta line represents a_{12}, and the blue dots represent $C_{I_{12}}$. The cyan lines/dots represent 11-component variables a_{11} and $C_{I_{11}}$, plotted for comparison purposes.

just like themselves, inversely proportional to their denominators, which are functions of the orientation components a_{11} and a_{12} respectively. So, if we calculate these proportionality quantities, and compare them by dividing one with another, we will then have the a contour plot shown in Figure B.2, with some considerable values of the ratio contoured. As shown by Figure B.2, when the fiber orientation stabilizes — likely when $a_{11} \in (0.65, 0.85)$, and $a_{12} \in (-0.2, 0.2)$, $C_{I_{12}}$ tends to have a deviation larger than $C_{I_{11}}$, possibly many times larger. And this poses a **precision** issue when using $C_{I_{12}}$ as C_I.

B.3 Conclusion

We use $C_{I_{11}}$ over $C_{I_{12}}$ as C_I in the thesis, for the following reasons:

(a) When the fibers align from a random orientation, $C_{I_{11}}$ quickly decreases and maintains a relatively small deviation.

(b) When the fibers align from a random orientation, $C_{I_{12}}$ quickly decreases as a_{12} peaks, then fluctuates as a_{12} decreases. When a_{12} drops back below 0.2, $C_{I_{12}}$ becomes more sensitive to the change of a_{12} than $C_{I_{11}}$ to a_{11}, causing much greater deviations, which makes it numerically difficult to produce a meaningful $C_{I_{12}}$.

In other words, if hypothetically, the range of a_{11} when the fiber orientation stabilizes was near 0.4–0.6, and $a_{12} > 0.3$, we would then choose $C_{I_{12}}$ over $C_{I_{11}}$ to use as C_I. Or assume that the deviation of these two quantities were of comparable orders, we would then consider alternative options to involve both of them in the calculation processes. But for now, because of the reasons listed above, we only include $C_{I_{11}}$ as the C_I throughout this thesis.

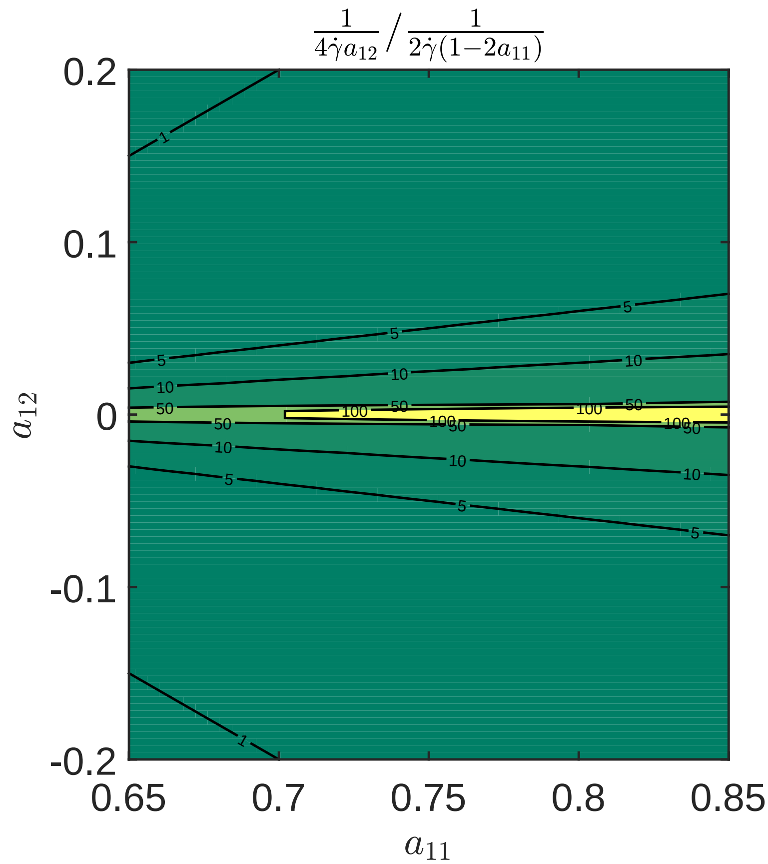

Figure B.2: A contour plot of $\frac{1}{4\dot{\gamma}a_{12}} / \frac{1}{2\dot{\gamma}(1-2a_{11})}$ when $a_{11} \in (0.65, 0.85)$, and $a_{12} \in (-0.2, 0.2)$. The deviation of $C_{I_{12}}$ becomes significantly greater than that of $C_{I_{11}}$ as the value of a_{12} decreases.

Appendix C

AVERAGED C_I CALCULATED FROM SIMULATION RESULTS

Table C.1: Average C_I^{fiber} calculated from simulations of neat fiber suspensions

C_I^{fiber}		vol%$_{\text{fiber}}$		
		7%	15%	20%
aspect ratio	18	0.0056	0.0073	0.0096
	20	0.0054	0.0068	0.0080
	22	0.0040	0.0053	0.0059

Table C.2: Average $C_I^{\text{fiber w/ particle}}$ calculated from simulations of hybrid fiber-particle suspensions

$C_I^{\text{fiber w/ particle}}$		vol%$_{\text{particle}}$					
		0	6%	8%	10%	12%	14%
aspect ratio	18	0.0073	0.0104	0.0111	0.0116	0.0135	0.0162
	20	0.0068	0.0089	0.0094	0.0097	0.0108	0.0123
	22	0.0053	0.0068	0.0080	0.0076	0.0089	0.0089

Appendix D

COPYRIGHT PERMISSIONS

Please refer to the following attachments for copyright permissions for [2, 1, 3, 40, 38].

Xiaoqing Li <xqingli@udel.edu>

RE: Submission Confirmation: Obtain Permission – Book request

1 message

Permissions Helpdesk <permissionshelpdesk@elsevier.com> Thu, Jan 28, 2016 at 12:03 PM
To: Xiaoqing Li <xqingli@udel.edu>

Dear Ms. Li:

According to our records, Elsevier no longer owns the rights to this volume as they have reverted to the author:

FLOW AND RHEOLOGY IN POLYMER COMPOSITES MANUFACTURING CMS 10	FLOW AND RHEOLOGY IN POLYMER COMPOSITES MANUFACTURING CMS 10	COMPOSITES MATERIALS SERIES, VOL.10	1000	ADVANI	2/3/1994

If Dr. Advani has approved of your reuse of this material, no further permission appears to be necessary.

Best of luck with your thesis and best regards,

Hop

Hop Wechsler

Permissions Helpdesk Manager

Elsevier

1600 John F. Kennedy Boulevard

Suite 1800

Philadelphia, PA 19103-2899

Tel: +1-215-239-3520

Mobile: +1-215-900-5674

Fax: +1-215-239-3805

E-mail: h.wechsler@elsevier.com

Contact the Permissions Helpdesk:

+1-800-523-4069 x 3808 *permissionshelpdesk@elsevier.com*

From: Xiaoqing Li [mailto:xqingli@udel.edu]
Sent: Thursday, January 28, 2016 12:59 PM
To: Permissions Helpdesk
Subject: Fwd: Submission Confirmation: Obtain Permission – Book request

---------- Forwarded message ----------
From: <permissions@elsevier.com>
Date: Thu, Jan 28, 2016 at 11:55 AM
Subject: Submission Confirmation: Obtain Permission – Book request
To: xqingli@udel.edu

Dear A Study of Fiber Orientation in Particle-Loaded Suspensions Using a Direct Simulation Method with Collision Strategy Li,

Thank you for your request.

The details are summarized below:

Title: A Study of Fiber Orientation in Particle-Loaded Suspensions Using a Direct Simulation Method with Collision Strategy Xiaoqing Li

Institute/company: University of Delaware
Address: 5002 Sheboygan Ave APT 206
Post/Zip Code: 53705

City: Madison
State/Territory: WI
Country: United States
Telephone: (302) 365-0427
Email: xqingli@udel.edu

Type of Publication: Book

Book Title:Flow and Rheology in Polymer Composites Manufacturing
Book ISBN: 978-0-444-89347-5
Book Author: Dr. Suresh G. Advani
Book Year: 1994
Book Pages: 148 to 149
Book Chapter number: 6
Book Chapter title: Processing of short-fiber systems

I would like to use: Figure(s)
Quantity of material: 1x Fig. 6.1 1x TABLE 6.1
Excerpts:
Are you the author of the Elsevier material? No
If not, is the Elsevier author involved? Yes
If yes, please provide details of how the Elsevier author is involved: Dr. Suresh G. Advani is the advisor on my Master's thesis, and the chair of my thesis committee.
In what format will you use the material? Electronic
Will you be translating the material? No
If yes, specify language:
Information about proposed use: Reuse in a thesis/dissertation
Proposed use text: My thesis will be "published" through UMI's dissertation program
Additional Comments / Information: I've made several contacts to request the permission of this material. But this is the first time I came across this platform. Please process this request by the end of Feb 1st, 2016 in Eastern Time when my defense happens. Thank you!

Kind regards,

Elsevier Permissions

--

Graduate Student

Mechanical Engineering

(302) 365-0427

University of Delaware

Xiaoqing Li <xqingli@udel.edu>

RE: Obtain Permission – Book request

Jones, Jennifer (ELS-OXF) <J.Jones@elsevier.com> Tue, Feb 2, 2016 at 10:04 AM
To: "xqingli@udel.edu" <xqingli@udel.edu>

ELSEVIER

Dear Xiaoqing Li

We hereby grant you permission to reprint the material detailed below at no charge **in your thesis** subject to the following conditions:

1. If any part of the material to be used (for example, figures) has appeared in our publication with credit or acknowledgement to another source, permission must also be sought from that source. If such permission is not obtained then that material may not be included in your publication/copies.

2. Suitable acknowledgment to the source must be made, either as a footnote or in a reference list at the end of your publication, as follows:

"This article was published in Publication title, Vol number, Author(s), Title of article, Page Nos, Copyright Elsevier (or appropriate Society name) (Year)."

3. Your thesis may be submitted to your institution in either print or electronic form.

4. Reproduction of this material is confined to the purpose for which permission is hereby given.

5. This permission is granted for non-exclusive world **English** rights only. For other languages please reapply separately for each one required. Permission excludes use in an electronic form other than submission. Should you have a specific electronic project in mind please reapply for permission

6. This includes permission for UMI to supply single copies, on demand, of the complete thesis.

Should your thesis be published commercially, please reapply for permission.

Yours sincerely

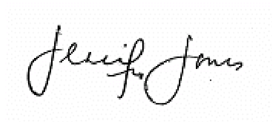

Jennifer Jones
Permissions Specialist

Elsevier Limited, a company registered in England and Wales with company number 1982084, whose registered office is The Boulevard, Langford Lane, Kidlington, Oxford, OX5 1GB, United Kingdom.

From: xqingli@udel.edu [mailto:xqingli@udel.edu]
Sent: 28 January 2016 17:55
To: Rights and Permissions (ELS)
Subject: Obtain Permission – Book request

Title: A Study of Fiber Orientation in Particle-Loaded Suspensions Using a Direct Simulation Method with Collision Strategy Xiaoqing Li

Institute/company: University of Delaware
Address: 5002 Sheboygan Ave APT 206
Post/Zip Code: 53705
City: Madison
State/Territory: WI
Country: United States
Telephone: (302) 365-0427
Email: xqingli@udel.edu

Type of Publication: Book

Book Title:Flow and Rheology in Polymer Composites Manufacturing
Book ISBN: 978-0-444-89347-5
Book Author: Dr. Suresh G. Advani
Book Year: 1994
Book Pages: 148 to 149
Book Chapter number: 6
Book Chapter title: Processing of short-fiber systems

I would like to use: Figure(s)
Quantity of material: 1x Fig. 6.1 1x TABLE 6.1
Excerpts:
Are you the author of the Elsevier material? No
If not, is the Elsevier author involved? Yes
If yes, please provide details of how the Elsevier author is involved: Dr. Suresh G. Advani is the advisor on my Master's thesis, and the chair of my thesis committee.
In what format will you use the material? Electronic
Will you be translating the material? No
If yes, specify language:
Information about proposed use: Reuse in a thesis/dissertation

Proposed use text: My thesis will be "published" through UMI's dissertation program
Additional Comments / Information: I've made several contacts to request the permission of this material. But this is the first time I came across this platform. Please process this request by the end of Feb 1st, 2016 in Eastern Time when my defense happens. Thank you!

THE ROYAL SOCIETY LICENSE
TERMS AND CONDITIONS

Jan 24, 2016

This Agreement between XIAOQING LI ("You") and The Royal Society ("The Royal Society") consists of your license details and the terms and conditions provided by The Royal Society and Copyright Clearance Center.

All payments must be made in full to CCC. For payment instructions, please see information listed at the bottom of this form.

License Number	3795670603384
License date	Jan 24, 2016
Licensed Content Publisher	The Royal Society
Licensed Content Publication	Philosophical Transactions A
Licensed Content Title	Technology of the 1990s: Advanced Materials and Predictive Design [and Discussion]
Licensed Content Author	M. F. Ashby,S. F. Bush,N. Swindells,R. Bullough,G. Ellison,Y. Lindblom,R. W. Cahn,J. F. Barnes
Licensed Content Date	1987-07-27
Licensed Content Volume Number	322
Licensed Content Issue Number	1567
Volume number	322
Issue number	1567
Type of Use	Thesis/Dissertation
Requestor type	academic/educational
Format	electronic
Portion	figures/tables/images
Quantity	1
Will you be translating?	no
Circulation	100
Order reference number	None
Title of your thesis / dissertation	A STUDY OF FIBER ORIENTATIONS IN PARTICLE-LOADED SUSPENSIONS USING A DIRECT SIMULATION METHOD WITH COLLISION STRATEGY
Expected completion date	Jan 2016
Estimated size (number of pages)	60
Requestor Location	XIAOQING LI 5002 SHEBOYGAN AVE APT 206

MADISON, WI 53705
United States
Attn: XIAOQING LI

Billing Type	Credit Card
Credit card info	American Express ending in 1662
Credit card expiration	10/2021
Total	3.50 USD

Terms and Conditions

STANDARD TERMS AND CONDITIONS FOR REPRODUCTION OF MATERIAL FROM A ROYAL SOCIETY JOURNAL

1. Use of the material is restricted to the type of use specified in your order details.
2. The publisher for this copyrighted material is the Royal Society. By clicking "accept" in connection with completing this licensing transaction, you agree that the following terms and conditions apply to this transaction (along with the Billing and Payment terms and conditions established by Copyright Clearance Center, Inc. ("CCC"), at the time that you opened your Rightslink account and that are available at any time at http://myaccount.copyright.com.
3. The following credit line appears wherever the material is used: author, title, journal, year, volume, issue number, pagination, by permission of the Royal Society.
4. For the reproduction of a full article from a Royal Society journal for whatever purpose, the corresponding author of the material concerned should be informed of the proposed use. Contact details for the corresponding authors of all Royal Society journals can be found alongside either the abstract or full text of the article concerned, accessible from royalsocietypublishing.org.
5. If the credit line in our publication indicates that any of the figures, images or photos was reproduced from an earlier source it will be necessary for you to clear this permission with the original publisher as well. If this permission has not been obtained, please note that this material cannot be included in your publication/photocopies.
6. Licenses may be exercised anywhere in the world.
7. While you may exercise the rights licensed immediately upon issuance of the license at the end of the licensing process for the transaction, provided that you have disclosed complete and accurate details of your proposed use, no license is finally effective unless and until full payment is received from you (either by publisher or by CCC) as provided in CCC's Billing and Payment terms and conditions. If full payment is not received on a timely basis, then any license preliminarily granted shall be deemed automatically revoked and shall be void as if never granted. Further, in the event that you breach any of these terms and conditions or any of CCC's Billing and Payment terms and conditions, the license is automatically revoked and shall be void as if never granted. Use of materials as described in a revoked license, as well as any use of the materials beyond the scope of an unrevoked license, may constitute copyright infringement and publisher reserves the right to take any and all action to protect its copyright in the materials.
8. Publisher reserves all rights not specifically granted in the combination of (i) the license details provided by you and accepted in the course of this licensing transaction, (ii) these terms and conditions and (iii) CCC's Billing and Payment terms and conditions.
9. Publisher makes no representations or warranties with respect to the licensed material.
10. You hereby indemnify and agree to hold harmless publisher and CCC, and their respective officers, directors, employees and agents, from and against any and all claims arising out of your use of the licensed material other than as specifically authorized pursuant

to this license.
11. This license may not be amended except in a writing signed by both parties (or, in the case of publisher, by CCC on publisher's behalf).

01/23/2016

PlastiComp, Inc.

110 Galewski Drive

Winona, MN 55987 USA

To whom this may concern:

I am a Master’s student at the University of Delaware. I am in the process of preparing a degree thesis to be "published" through UMI's dissertation program and am seeking permission to include the graphic material in my publication from the following link:.
http://www.appliancedesign.com/articles/94628-boosting-performance-without-breaking-the-bank

The title of my thesis is:

A study of fiber orientations in particle-loaded suspensions using a direct simulation method with collision strategy

If the permission is granted, your graphs will be credited and acknowledged, and they will be included in my thesis as shown below:

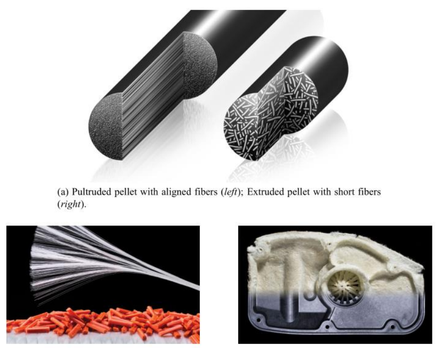

(a) Pultruded pellet with aligned fibers (*left*); Extruded pellet with short fibers (*right*).

(b) Continuous strands of fiber (*top*); Resulting long fiber reinforced thermoplastic pellets (*bottom*).

(c) Internal fiber skeleton of long-fiber reinforced composite part (*tophalf*); Long-fiber reinforced composite part (*botttomhalf*).

Figure 1.2: (a) A diagram of long- and short- fiber reinforced composite pellets; (b) An actual photo of fiber strands and resulting pellets; (c) An example of the injection-molded part compared with its fiber skeleton.

Please let me know if it is ok for me to use this work in this manner.

Please indicate your approval of this request by signing the letter where indicated below and returning it to me as soon as possible using the self-addressed envelope. Your signing of this letter will also confirm that you own the copyright to the above-described material.

Very truly yours,
Xiaoqing Li
Master's student in Mechanical Engineering
University of Delaware
xqingli@udel.edu
(302) 365-0427

For copyright owner use:

PERMISSION GRANTED FOR THE USE REQUESTED ABOVE:

Permission to publish photographs and illustrations detail above is hereby granted for educational research purposes, all copyrights are retained by PlastiComp, Inc. and not transferred. Please credit "PlastiComp, Inc." as source for these images.

By: Kirk Fratzke

Title: Media marketing coordinator
PlastiComp, Inc.
110 Galewski Dr
Winona, MN 55987
507-474-0197

Date: January 25, 2015

The preferred source of your graphics, if other than the one before:

Xiaoqing Li <xqingli@udel.edu>

RE: Permission request to reprint the journal content in my Master's thesis

1 message

Hyun Wook Jung <hwjung@grtrkr.korea.ac.kr> Sun, Jan 24, 2016 at 7:47 PM
To: xqingli@udel.edu
Cc: mschun@kist.re.kr

Dear Xiaoqing Li,

On behalf of the current Editor-in-Chief of KARJ, Dr. Myung-Suk Chun, I am sending e-mail to you. (Now, I am an associate Editor.)

You can use Figs. 1 and 3 of Prof. Hwang's article published in KARJ. Please, do not forget to mention the copyright permission when you use these figures.

Best regards.

Hyun Wook Jung

Hyun Wook Jung, Professor

Department of Chemical and Biological Engineering

Korea University

Anam-dong, Seongbuk-gu, Seoul 136-713, Korea

Tel: 82-2-3290-3306

E-mail: hwjung@grtrkr.korea.ac.kr

From: 유변학회 [mailto:ksr@ksr.or.kr]
Sent: Monday, January 25, 2016 9:58 AM
To: 정현욱
Cc: 전명석
Subject: 유변: Permission request to reprint the journal content in my Master's thesis

---------------------(아래) ---------------------------

From: Xiaoqing Li [mailto:xqingli@udel.edu]
Sent: Sunday, January 24, 2016 6:05 PM
To: ksr@ksr.or.kr
Subject: Permission request to reprint the journal content in my Master's thesis

Dear Korean Society of Rheology,

I am a Master's student at the University of Delaware. I am in the process of preparing a degree thesis to be "published" through UMI's dissertation program and am seeking permission to include the figure material in my publication from the following journal paper:

H. Chung, S. Kang, and W. R. Hwang, "Numerical simulations of elliptic particle suspensions in sliding bi-periodic frames," Korea-Australia Rheology Journal, vol. 17, no. 4, pp. 171–180, 2005.

This paper is too old to be available on Springer.com, hence I'm writing to you.

The title of my thesis is:

A study of fiber orientations in particle-loaded suspensions using a direct simulation method with collision strategy

If the permission is granted, Fig. 1 and Fig. 3 will be credited, acknowledged and properly cited. And they will be included in my thesis.

Please let me know if it is ok for me to use this work in this manner.

If so, please kindly finished and return the attached files (in pdf or doc format) to me at xqingli@udel.edu

If this is not the appropriate way to obtain permission of copyrighted content, please direct me to the correct department.

Sincerely,

Xiaoqing Li

--

Graduate Student

Mechanical Engineering

(302) 365-0427

University of Delaware

ELSEVIER LICENSE
TERMS AND CONDITIONS

Jan 23, 2016

This is a License Agreement between XIAOQING LI ("You") and Elsevier ("Elsevier") provided by Copyright Clearance Center ("CCC"). The license consists of your order details, the terms and conditions provided by Elsevier, and the payment terms and conditions.

All payments must be made in full to CCC. For payment instructions, please see information listed at the bottom of this form.

Supplier	Elsevier Limited The Boulevard,Langford Lane Kidlington,Oxford,OX5 1GB,UK
Registered Company Number	1982084
Customer name	XIAOQING LI
Customer address	5002 SHEBOYGAN AVE APT 206
	MADISON, WI 53705
License number	3794990647453
License date	Jan 23, 2016
Licensed content publisher	Elsevier
Licensed content publication	Journal of Computational Physics
Licensed content title	Direct simulation of particle suspensions in sliding bi-periodic frames
Licensed content author	Wook Ryol Hwang,Martien A. Hulsen,Han E.H. Meijer
Licensed content date	1 March 2004
Licensed content volume number	194
Licensed content issue number	2
Number of pages	31
Start Page	742
End Page	772
Type of Use	reuse in a thesis/dissertation
Portion	figures/tables/illustrations
Number of figures/tables/illustrations	3
Format	electronic
Are you the author of this Elsevier article?	No
Will you be translating?	No
Original figure numbers	figure 1, 4
Title of your	A STUDY OF FIBER ORIENTATIONS IN PARTICLE-LOADED

thesis/dissertation	SUSPENSIONS USING A DIRECT SIMULATION METHOD WITH COLLISION STRATEGY
Expected completion date	Jan 2016
Estimated size (number of pages)	60
Elsevier VAT number	GB 494 6272 12
Permissions price	0.00 USD
VAT/Local Sales Tax	0.00 USD / 0.00 GBP
Total	0.00 USD
Terms and Conditions	

INTRODUCTION

1. The publisher for this copyrighted material is Elsevier. By clicking "accept" in connection with completing this licensing transaction, you agree that the following terms and conditions apply to this transaction (along with the Billing and Payment terms and conditions established by Copyright Clearance Center, Inc. ("CCC"), at the time that you opened your Rightslink account and that are available at any time at http://myaccount.copyright.com).

GENERAL TERMS

2. Elsevier hereby grants you permission to reproduce the aforementioned material subject to the terms and conditions indicated.
3. Acknowledgement: If any part of the material to be used (for example, figures) has appeared in our publication with credit or acknowledgement to another source, permission must also be sought from that source. If such permission is not obtained then that material may not be included in your publication/copies. Suitable acknowledgement to the source must be made, either as a footnote or in a reference list at the end of your publication, as follows:
"Reprinted from Publication title, Vol /edition number, Author(s), Title of article / title of chapter, Pages No., Copyright (Year), with permission from Elsevier [OR APPLICABLE SOCIETY COPYRIGHT OWNER]." Also Lancet special credit - "Reprinted from The Lancet, Vol. number, Author(s), Title of article, Pages No., Copyright (Year), with permission from Elsevier."
4. Reproduction of this material is confined to the purpose and/or media for which permission is hereby given.
5. Altering/Modifying Material: Not Permitted. However figures and illustrations may be altered/adapted minimally to serve your work. Any other abbreviations, additions, deletions and/or any other alterations shall be made only with prior written authorization of Elsevier Ltd. (Please contact Elsevier at permissions@elsevier.com)
6. If the permission fee for the requested use of our material is waived in this instance, please be advised that your future requests for Elsevier materials may attract a fee.
7. Reservation of Rights: Publisher reserves all rights not specifically granted in the combination of (i) the license details provided by you and accepted in the course of this licensing transaction, (ii) these terms and conditions and (iii) CCC's Billing and Payment terms and conditions.
8. License Contingent Upon Payment: While you may exercise the rights licensed immediately upon issuance of the license at the end of the licensing process for the transaction, provided that you have disclosed complete and accurate details of your proposed use, no license is finally effective unless and until full payment is received from you (either by publisher or by CCC) as provided in CCC's Billing and Payment terms and conditions. If

full payment is not received on a timely basis, then any license preliminarily granted shall be deemed automatically revoked and shall be void as if never granted. Further, in the event that you breach any of these terms and conditions or any of CCC's Billing and Payment terms and conditions, the license is automatically revoked and shall be void as if never granted. Use of materials as described in a revoked license, as well as any use of the materials beyond the scope of an unrevoked license, may constitute copyright infringement and publisher reserves the right to take any and all action to protect its copyright in the materials.
9. Warranties: Publisher makes no representations or warranties with respect to the licensed material.
10. Indemnity: You hereby indemnify and agree to hold harmless publisher and CCC, and their respective officers, directors, employees and agents, from and against any and all claims arising out of your use of the licensed material other than as specifically authorized pursuant to this license.
11. No Transfer of License: This license is personal to you and may not be sublicensed, assigned, or transferred by you to any other person without publisher's written permission.
12. No Amendment Except in Writing: This license may not be amended except in a writing signed by both parties (or, in the case of publisher, by CCC on publisher's behalf).
13. Objection to Contrary Terms: Publisher hereby objects to any terms contained in any purchase order, acknowledgment, check endorsement or other writing prepared by you, which terms are inconsistent with these terms and conditions or CCC's Billing and Payment terms and conditions. These terms and conditions, together with CCC's Billing and Payment terms and conditions (which are incorporated herein), comprise the entire agreement between you and publisher (and CCC) concerning this licensing transaction. In the event of any conflict between your obligations established by these terms and conditions and those established by CCC's Billing and Payment terms and conditions, these terms and conditions shall control.
14. Revocation: Elsevier or Copyright Clearance Center may deny the permissions described in this License at their sole discretion, for any reason or no reason, with a full refund payable to you. Notice of such denial will be made using the contact information provided by you. Failure to receive such notice will not alter or invalidate the denial. In no event will Elsevier or Copyright Clearance Center be responsible or liable for any costs, expenses or damage incurred by you as a result of a denial of your permission request, other than a refund of the amount(s) paid by you to Elsevier and/or Copyright Clearance Center for denied permissions.

LIMITED LICENSE

The following terms and conditions apply only to specific license types:
15. **Translation**: This permission is granted for non-exclusive world **English** rights only unless your license was granted for translation rights. If you licensed translation rights you may only translate this content into the languages you requested. A professional translator must perform all translations and reproduce the content word for word preserving the integrity of the article.
16. **Posting licensed content on any Website**: The following terms and conditions apply as follows: Licensing material from an Elsevier journal: All content posted to the web site must maintain the copyright information line on the bottom of each image; A hyper-text must be included to the Homepage of the journal from which you are licensing at http://www.sciencedirect.com/science/journal/xxxxx or the Elsevier homepage for books at http://www.elsevier.com; Central Storage: This license does not include permission for a scanned version of the material to be stored in a central repository such as that provided by Heron/XanEdu.

Licensing material from an Elsevier book: A hyper-text link must be included to the Elsevier homepage at http://www.elsevier.com . All content posted to the web site must maintain the copyright information line on the bottom of each image.

Posting licensed content on Electronic reserve: In addition to the above the following clauses are applicable: The web site must be password-protected and made available only to bona fide students registered on a relevant course. This permission is granted for 1 year only. You may obtain a new license for future website posting.
17. **For journal authors:** the following clauses are applicable in addition to the above:
Preprints:
A preprint is an author's own write-up of research results and analysis, it has not been peer-reviewed, nor has it had any other value added to it by a publisher (such as formatting, copyright, technical enhancement etc.).
Authors can share their preprints anywhere at any time. Preprints should not be added to or enhanced in any way in order to appear more like, or to substitute for, the final versions of articles however authors can update their preprints on arXiv or RePEc with their Accepted Author Manuscript (see below).
If accepted for publication, we encourage authors to link from the preprint to their formal publication via its DOI. Millions of researchers have access to the formal publications on ScienceDirect, and so links will help users to find, access, cite and use the best available version. Please note that Cell Press, The Lancet and some society-owned have different preprint policies. Information on these policies is available on the journal homepage.
Accepted Author Manuscripts: An accepted author manuscript is the manuscript of an article that has been accepted for publication and which typically includes author-incorporated changes suggested during submission, peer review and editor-author communications.
Authors can share their accepted author manuscript:

- immediately
  - via their non-commercial person homepage or blog
  - by updating a preprint in arXiv or RePEc with the accepted manuscript
  - via their research institute or institutional repository for internal institutional uses or as part of an invitation-only research collaboration work-group
  - directly by providing copies to their students or to research collaborators for their personal use
  - for private scholarly sharing as part of an invitation-only work group on commercial sites with which Elsevier has an agreement
- after the embargo period
  - via non-commercial hosting platforms such as their institutional repository
  - via commercial sites with which Elsevier has an agreement

In all cases accepted manuscripts should:

- link to the formal publication via its DOI
- bear a CC-BY-NC-ND license - this is easy to do
- if aggregated with other manuscripts, for example in a repository or other site, be shared in alignment with our hosting policy not be added to or enhanced in any way to appear more like, or to substitute for, the published journal article.

Published journal article (JPA): A published journal article (PJA) is the definitive final record of published research that appears or will appear in the journal and embodies all value-adding publishing activities including peer review co-ordination, copy-editing, formatting, (if relevant) pagination and online enrichment.

Policies for sharing publishing journal articles differ for subscription and gold open access articles:

Subscription Articles: If you are an author, please share a link to your article rather than the full-text. Millions of researchers have access to the formal publications on ScienceDirect, and so links will help your users to find, access, cite, and use the best available version. Theses and dissertations which contain embedded PJAs as part of the formal submission can be posted publicly by the awarding institution with DOI links back to the formal publications on ScienceDirect.

If you are affiliated with a library that subscribes to ScienceDirect you have additional private sharing rights for others' research accessed under that agreement. This includes use for classroom teaching and internal training at the institution (including use in course packs and courseware programs), and inclusion of the article for grant funding purposes.

Gold Open Access Articles: May be shared according to the author-selected end-user license and should contain a CrossMark logo, the end user license, and a DOI link to the formal publication on ScienceDirect.

Please refer to Elsevier's posting policy for further information.

18. **For book authors** the following clauses are applicable in addition to the above: Authors are permitted to place a brief summary of their work online only. You are not allowed to download and post the published electronic version of your chapter, nor may you scan the printed edition to create an electronic version. **Posting to a repository:** Authors are permitted to post a summary of their chapter only in their institution's repository.

19. **Thesis/Dissertation**: If your license is for use in a thesis/dissertation your thesis may be submitted to your institution in either print or electronic form. Should your thesis be published commercially, please reapply for permission. These requirements include permission for the Library and Archives of Canada to supply single copies, on demand, of the complete thesis and include permission for Proquest/UMI to supply single copies, on demand, of the complete thesis. Should your thesis be published commercially, please reapply for permission. Theses and dissertations which contain embedded PJAs as part of the formal submission can be posted publicly by the awarding institution with DOI links back to the formal publications on ScienceDirect.

Elsevier Open Access Terms and Conditions

You can publish open access with Elsevier in hundreds of open access journals or in nearly 2000 established subscription journals that support open access publishing. Permitted third party re-use of these open access articles is defined by the author's choice of Creative Commons user license. See our open access license policy for more information.

Terms & Conditions applicable to all Open Access articles published with Elsevier:

Any reuse of the article must not represent the author as endorsing the adaptation of the article nor should the article be modified in such a way as to damage the author's honour or reputation. If any changes have been made, such changes must be clearly indicated.

The author(s) must be appropriately credited and we ask that you include the end user license and a DOI link to the formal publication on ScienceDirect.

If any part of the material to be used (for example, figures) has appeared in our publication with credit or acknowledgement to another source it is the responsibility of the user to ensure their reuse complies with the terms and conditions determined by the rights holder.

Additional Terms & Conditions applicable to each Creative Commons user license:

CC BY: The CC-BY license allows users to copy, to create extracts, abstracts and new

works from the Article, to alter and revise the Article and to make commercial use of the Article (including reuse and/or resale of the Article by commercial entities), provided the user gives appropriate credit (with a link to the formal publication through the relevant DOI), provides a link to the license, indicates if changes were made and the licensor is not represented as endorsing the use made of the work. The full details of the license are available at http://creativecommons.org/licenses/by/4.0.
CC BY NC SA: The CC BY-NC-SA license allows users to copy, to create extracts, abstracts and new works from the Article, to alter and revise the Article, provided this is not done for commercial purposes, and that the user gives appropriate credit (with a link to the formal publication through the relevant DOI), provides a link to the license, indicates if changes were made and the licensor is not represented as endorsing the use made of the work. Further, any new works must be made available on the same conditions. The full details of the license are available at http://creativecommons.org/licenses/by-nc-sa/4.0.
CC BY NC ND: The CC BY-NC-ND license allows users to copy and distribute the Article, provided this is not done for commercial purposes and further does not permit distribution of the Article if it is changed or edited in any way, and provided the user gives appropriate credit (with a link to the formal publication through the relevant DOI), provides a link to the license, and that the licensor is not represented as endorsing the use made of the work. The full details of the license are available at http://creativecommons.org/licenses/by-nc-nd/4.0.
Any commercial reuse of Open Access articles published with a CC BY NC SA or CC BY NC ND license requires permission from Elsevier and will be subject to a fee.
Commercial reuse includes:

- Associating advertising with the full text of the Article
- Charging fees for document delivery or access
- Article aggregation
- Systematic distribution via e-mail lists or share buttons

Posting or linking by commercial companies for use by customers of those companies.

20. **Other Conditions**:

v1.8

Questions? customercare@copyright.com or +1-855-239-3415 (toll free in the US) or +1-978-646-2777.